



**INTERNATIONAL  
MATERIALS  
HANDLING  
CONFERENCE**

## ***BELTCON 3***

Some aspects of Surface Friction, Adhesion  
and Wear in the Gravity Flow, Handling and  
Belt Conveying of Bulk Solids

Prof A Roberts

***9, 10 & 11 September, 1985  
Landdrost Hotel  
Johannesburg***

***The S.A. Institute of Materials Handling  
The S.A. Institution of Mechanical Engineers  
The Materials Handling Research Group (University of the Witwatersrand)***

SOME ASPECTS OF SURFACE FRICTION, ADHESION AND WEAR  
IN THE GRAVITY FLOW, HANDLING AND BELT CONVEYING  
OF BULK SOLIDS

by

A.W. Roberts<sup>1</sup> and M. Ooms<sup>2</sup>

The University of Newcastle, Australia

SUMMARY

This paper examines the surface friction, adhesion and wear characteristics for bulk solids in motion against hopper, chute and feeder walls and in contact with conveyor belts. In hopper design, wall friction has a significant influence on the flow patterns generated and gravity flow performance. While reliable gravity flow in hoppers requires low wall friction, it is inevitable that wear will take place. Procedures are presented for determining specific wear in bins indicating zones of high potential wear and where hopper linings may need to be made thicker. A method to predict the wear characteristics of chutes and feeders is also presented. The interaction of bulk solids with conveyor belt surfaces is examined with specific reference to adhesion and belt surface roughness. The relevance to belt cleaning and bulk solid carry-over is discussed.

<sup>1</sup> Professor and Head, Department of Mechanical Engineering,  
Dean, Faculty of Engineering.

<sup>2</sup> Professional Officer, Department of Mechanical Engineering.

## 1. INTRODUCTION

The various mining, mineral and processing industries throughout the world rely heavily on bulk materials handling operations. Such operations include storage, gravity flow, feeding and transportation. With respect to the latter, belt conveyors play a major role, both for in-plant and over-land movement of materials. The costs associated with the handling of bulk materials are quite substantial and, in many cases, constitute a major proportion of the final product cost. For this reason, it is important that bulk materials handling plant be designed and operated with a view to obtaining high efficiency and reliability coupled with maximum economy. As a part of this goal, it is necessary to ensure that the plant is designed correctly so that continuous operation without flow blockages is assured and that problems due to wear and spillages are minimised.

In order that the foregoing objectives may be realised, it is particularly important that the flow properties of the bulk solid be determined for all expected operating conditions. The principal flow properties of direct concern are bulk strength and wall or surface friction with the latter having a major influence. The constrained motion of bulk solids in bins, feeders and transfer chutes and the movement of bulk materials by conveyor belts requires a detailed knowledge of the surface friction and adhesion characteristics of bulk solids in contact with hopper, chute and belt surfaces.

In hoppers, feeders and chutes a knowledge of the surface friction and adhesion characteristics will, for the chosen lining material, enable correct slope angles to be determined to ensure reliable flow. At the same time the friction characteristics, coupled with feedrates and normal pressures generated permit wear patterns to be predicted. In the case of conveyor belts, the friction and adhesion characteristics of bulk solids in contact with belt surfaces indicate the degree of difficulty of belt cleaning; through a better understanding of the bulk solid and belt surface interaction, the degree and selection of belt cleaners for efficient, reliable operation is possible.

The purpose of this paper is to highlight the problems of surface friction, adhesion and wear in gravity flow, feeding and conveying of bulk solids. Attention is given to gravity flow storage bins, feeders and chutes which are important components in bulk solid handling and belt conveying systems. Attention is also given to fundamental aspects of belt cleaning based on bulk solid/belt interaction, equipment design and carry-over considerations.

In evaluating the influences of surface friction and adhesion characteristics of bulk solids in contact with hopper and chute walls and with conveyor belts, it is important that the relevant parameters be examined. Such parameters as surface roughness, particle size distribution, moisture content and contact time are shown to have a significant influence. Consideration of these parameters on the friction and adhesion characteristics of bulk solids in contact with surfaces is also given in the paper.

## 2. CONCEPTS OF BIN DESIGN

The general theory pertaining to the gravity flow of bulk solids in hoppers and the associated design procedure are fully documented [1-3]. However, for the purpose of the present discussion, the salient aspects of the bin design philosophy will be briefly reviewed.

### 2.1 Bin Flow Patterns

As is now widely known there are two basic modes of flow in symmetrical bins, mass flow and funnel flow.

In mass flow the bulk solid is in motion at substantially every point in the bin whenever material is drawn from the outlet. It is a "first-in, first-out" flow pattern. The bulk solid flows along the walls with the bin and hopper (that is the tapered section of the bin) forming the flow channel. Mass flow is the ideal flow pattern when reliable flow is required and the bin needs to be self cleaning. Mass flow occurs when the hopper walls are sufficiently steep and smooth and there are no abrupt transitions or inflowing valleys. Since the flow occurs along the bin walls, mass flow bins are prone to abrasive wear.

Funnel flow occurs when the bulk solid sloughs off the surface and discharges through a vertical channel which forms within the bulk solid in the bin. It is a "first-in, last-out" mode of flow which occurs when the hopper walls are rough and the hopper half-angle  $\alpha$  is too large. The flow tends to be erratic with a strong tendency to form stable pipes which obstruct bin discharge. The live capacity of funnel flow bins may be significantly limited. While funnel flow may be an undesirable flow pattern in many instances it does have the advantage of minimising bin wear.

Mass flow bins are classified according to the hopper shape and associated flow pattern. The two main types are conical hoppers, which operate with axi-symmetric flow, and wedge-shaped or chisel-shaped in which

plane flow occurs. In plane flow bins the hopper half-angle  $\alpha$  will usually be, on average, approximately  $10^\circ$  larger than that for the corresponding conical hoppers. Therefore, they offer larger storage capacity for the same head room than the conical bin but this advantage is somewhat offset by the long slotted opening which can cause feed problems.

## 2.2 Bulk Solid Parameters

For bin and chute design a knowledge of the bulk strength and hopper wall friction characteristics is of importance. These bulk solid parameters must be related to the desired flow modes developed in the particular flow channels formed by hoppers and chutes. The relevant details are depicted in Figure 1; Figures 1(a) and 1(b) show the flow channels in hoppers and chutes respectively while Figure 1(c) shows the bulk solid yield functions. The bulk strength, given by the Flow Function, is the unconfined yield strength  $\sigma_c$  expressed as a function of the major consolidation pressure  $\sigma_1$ .  $\sigma_c$  and  $\sigma_1$  are defined by the yield locus, Y.L., as indicated in Figure 1(c). The Effective Yield Locus, E.Y.L., defines the effective angle of internal friction  $\delta$ . The yield loci obtained for a range of values of  $\sigma_1$  permits the Flow Function to be obtained.

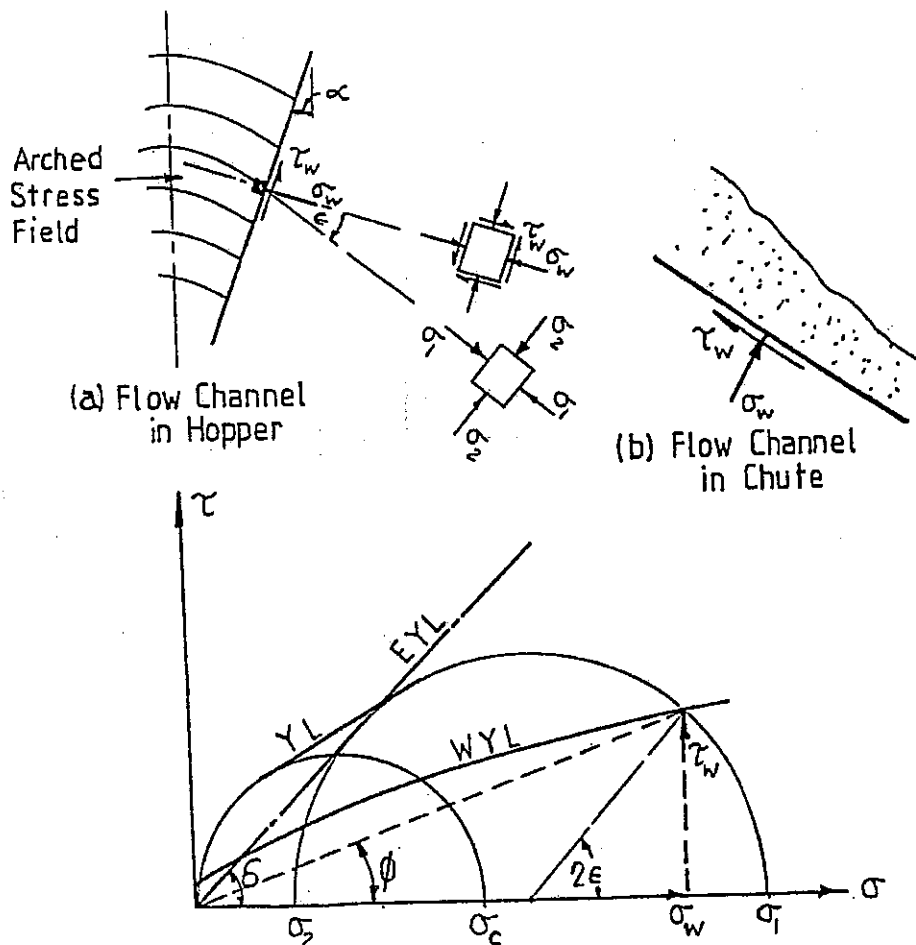


Figure 1 Bulk Solid Yield Loci and Flow Channels

Hopper wall surface friction governs the motion of a bulk solid relative to the hopper wall. Wall friction is defined by the wall yield loci, W.Y.L. Typically the W.Y.L. for most wall materials are slightly convex as shown in Figure 1. In some cases the W.Y.L. does not pass through the origin, indicating adhesion forces of attraction between the bulk solid and the wall surface. This is highlighted in Figure 2 which shows, diagrammatically, the low pressure end of the W.Y.L.; for illustrated purposes the W.Y.L. is shown extended into the tensile normal stress region. The adhesion effects are indicated by the adhesive stress  $\sigma_0$  which is the tensile stress in the absence of shear and the cohesive stress  $\tau_0$  which is the shear stress in the absence of normal stress.

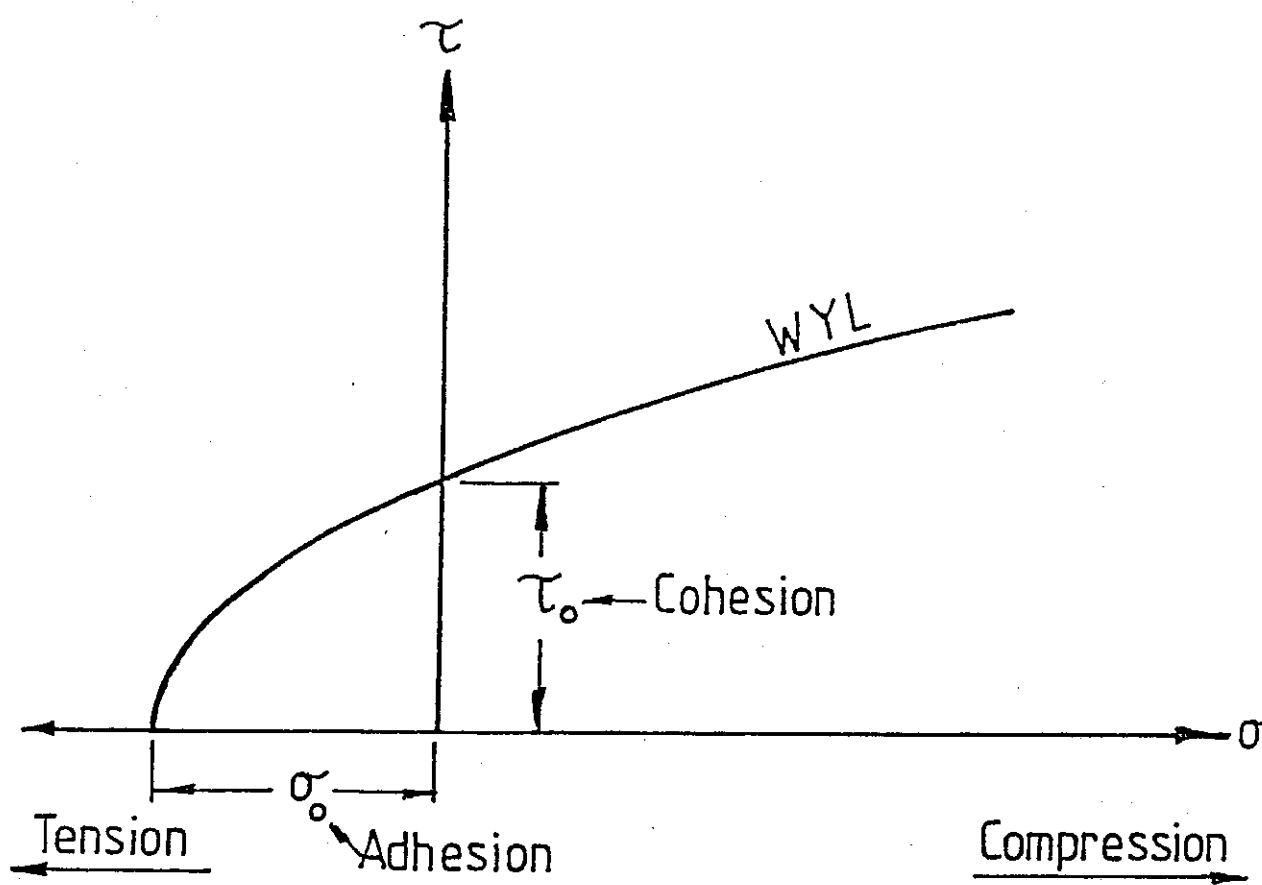


Figure 2 Adhesive Characteristics of the Surface or Wall Yield Locus

The wall friction angle is given by

$$\phi = \tan^{-1} \left( \frac{\tau_w}{\sigma_w} \right) \quad (1)$$

where  $\tau_w$  = shear stress at the wall

$\sigma_w$  = pressure acting normal to the wall.

It is evident from Figure 1 that as the normal pressure  $\sigma_w$  increases, the wall friction angle decreases, this being illustrated in Figure 3. At low values of  $\sigma_w$  the friction angle  $\phi$  can be very high, significantly influencing the geometry of mass flow hoppers in the region of the outlet and the performance of gravity flow chutes and belt cleaning devices. These latter influences of the wall friction characteristics is discussed in Sections 7 and 8.

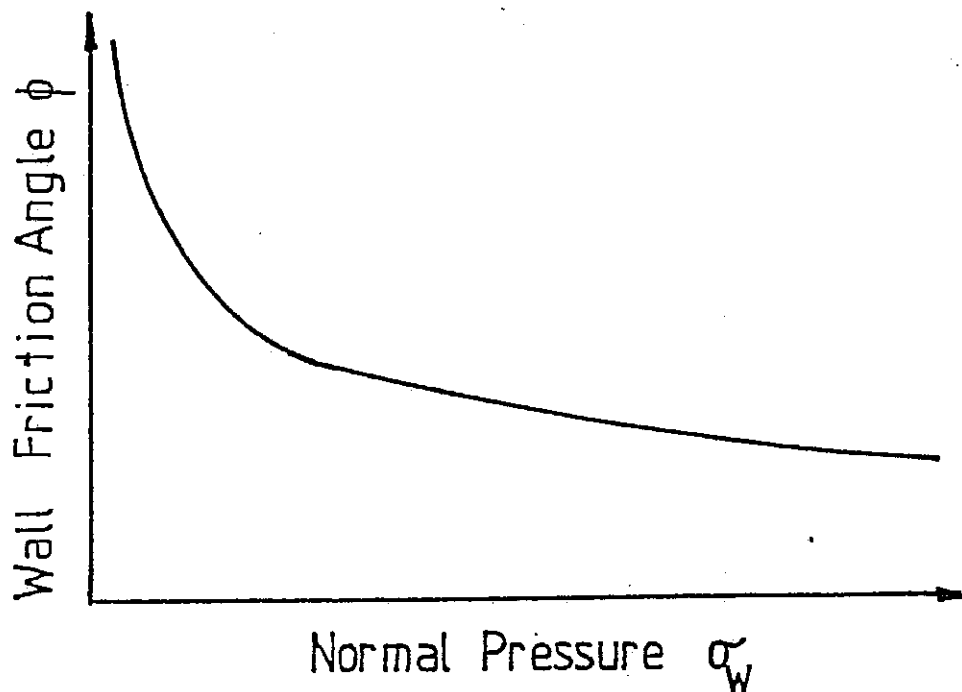


Figure 3 Characteristic Surface or Wall Friction Variation with Normal Pressure

For hopper design the wall friction angle  $\phi$  needs to be related to the major consolidation pressure  $\sigma_1$ . The relationship is depicted in Figure 1.

### 2.3 Limits for Mass Flow - Influence of Wall Friction

The limits for mass flow and funnel flow for both conical and plane flow channels have been established by Jenike [1,2]. These limits depend on the hopper half-angle  $\alpha$ , the wall friction angle  $\phi$  and the effective angle of internal friction  $\delta$ . For conical hoppers the limits for mass flow are well defined whereas for plane flow hoppers the limits are less severe [3].

Once the wall friction angle  $\phi$  and the effective angle of internal friction  $\delta$  have been obtained, the hopper half-angle  $\alpha$  may be determined.

In functional form

$$\alpha = f_1 (\phi, \delta) \quad (2)$$

Consider, for example, a conical hopper handling coal with  $\delta = 45^\circ$ . If the hopper is of mild steel it is subject to corrosion, the angle  $\phi$  is likely to be approximately  $30^\circ$ . On this basis,  $\alpha = 10^\circ$  which makes for a very steep hopper. If the hopper is lined with stainless steel, the friction angle  $\phi$  is likely to be approximately  $20^\circ$ . On this basis  $\alpha = 23^\circ$ . The corresponding angles for plane flow are  $\alpha = 22^\circ$  for  $\phi = 30^\circ$  and  $\alpha = 35^\circ$  for  $\phi = 20^\circ$ .

The importance of the wall friction angle  $\phi$  in determining the mode of flow is clearly demonstrated. For a given hopper geometry a small increase in  $\phi$  can change a conical hopper operating under mass flow into a conical hopper producing funnel flow.

#### 2.4 Critical Arching Dimension

For mass flow design it is important to ensure that a cohesive arch will not form anywhere within the hopper. While invariably, bulk solids gain strength with increase in consolidation pressure, most bulk solids tend towards a limiting strength. For this reason the critical location for arching normally occurs at the hopper outlet. Two parameters are important: firstly the 'Flow Function' FF representing the strength of the material as previously described and, secondly, the 'flow factor' ff which describes the stress condition in the hopper during flow.

In functional form the initial opening dimension B is given by

$$B = f_2 (\delta, \alpha, \phi, \sigma, \rho) \quad (3)$$

where  $\rho$  = bulk density, the other parameters being as previously defined. Details of the method used to determine B are given in References [1-3].

#### 2.5 Funnel Flow and Expanded Flow Geometry

As previously indicated, an attractive feature of funnel flow is the protection it offers to abrasive wear of bin and hopper walls. However this mode of flow generally limits, significantly, the live capacity of the bin. The performance of the bin in terms of draw-down and live capacity depends on the size of the bin opening dimension in relation to the critical pipe or rat-hole diameter  $D_f$  [2,3].

In functional form  $D_f$  is expressed as

$$D = f_3 (\sigma_1, \phi_t, \phi, \rho, h/D) \quad (4)$$

where the parameters not previously defined are

$\phi_t$  = static angle of internal friction

$h/D$  = bin height to diameter or width aspect ratio.

The method of determining  $D_f$  is given in References [2,3].

In order to completely empty a funnel flow bin it is necessary for the bin opening dimension  $B$  to be at least equal to the critical pipe dimension  $D_f$  corresponding to the maximum consolidation pressure. For many cohesive bulk solids under the normal range of consolidation pressures experienced during storage, critical pipe diameters several metres in magnitude are determined. In such cases funnel flow is not a practical solution.

Where large quantities of a bulk solid are to be stored, the expanded flow bin, as illustrated in Figure 4 offers considerable advantages. The bin combines the storage efficiency of the funnel flow bin with the reliable discharge characteristics of the mass flow hopper. It is necessary for the mass flow hopper to have a diameter at least equal to the critical pipe dimension  $D_f$  at the transition with the funnel flow section of the bin. This ensures that the flow of material from the funnel flow upper section of the bin can be fully expanded into the mass flow hopper. The expanded flow bin permits head heights for a given storage volume to be limited as well as providing wear protection to the main upper storage capacity. Wear is confined mainly to the mass flow hopper outlet when flow along the walls is necessary in order to obtain reliable discharge. The expanded flow bin concept may also be used to advantage in the case of bins or bunkers with multiple outlets.

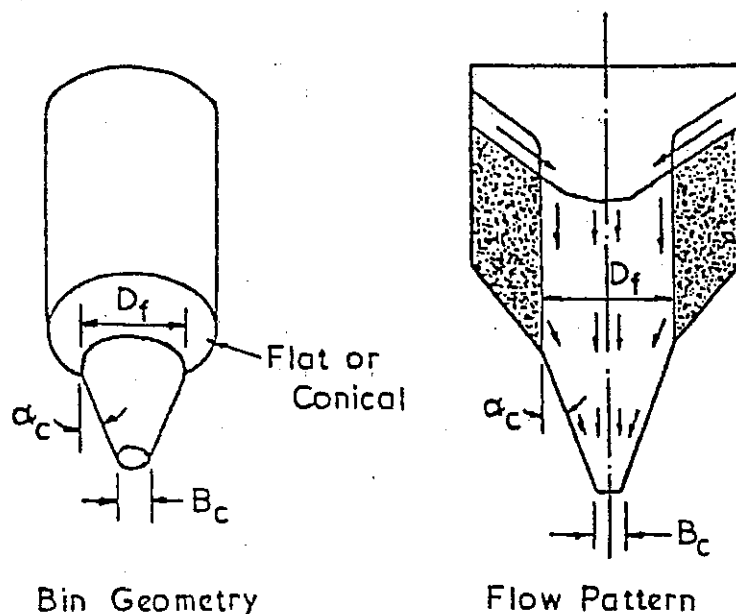


Figure 4 Expanded Flow Bin

### 3. BULK SOLID WALL FRICTION AND ROUGHNESS CHARACTERISTICS

Wall friction has a particularly significant influence on the performance and wear life of bulk handling plant. As shown by Roberts et al [4,5], and Ooms and Roberts [6-9] wall friction depends on the interaction between the bulk solid properties with those of the wall material. The relevant properties may be summarised:

- (i) Bulk Solid Properties - These include particle size distribution, moisture content, temperature, hardness, undisturbed storage time and chemical composition.
- (ii) Wall Material Properties - These include surface hardness, surface roughness, chemical composition and wall vibrations.

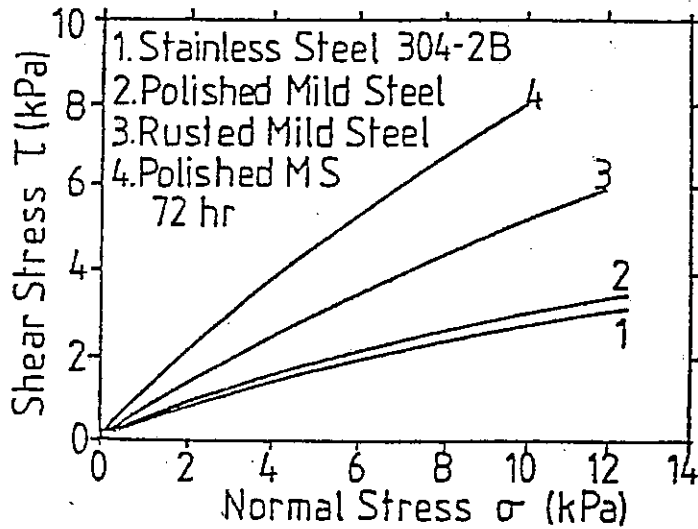
#### 3.1 Surface or Wall Friction

Some typical wall friction graphs are shown in Figure 5. Figure 5(a) shows the wall yield loci for black coal at 10% moisture content on stainless steel type 304 with 2B finish, mild steel polished and rusted mild steel for the instantaneous or zero storage time condition, as well as the polished mild steel surface after 72 hours undisturbed storage. The increase in friction in the latter case is quite considerable with corrosion and adhesion or bonding of coal particles to the steel surface occurring.

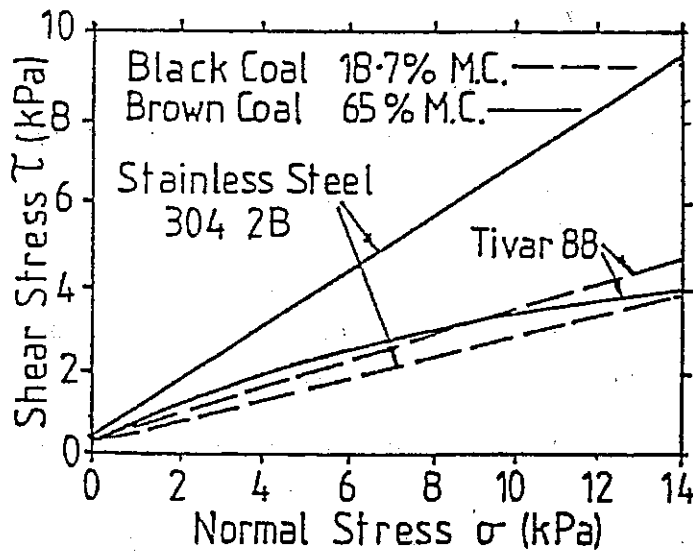
Figure 5(b) compares the wall yield loci for black coal at 18.7% moisture content and brown coal at 65% moisture content on two surfaces, stainless steel type 304 with 2B finish and Tivar 88, a ultra high molecular weight glass filled polyethylene material. While in absolute terms the moisture contents of the two coals are significantly different, in relative terms with respect to their composition and saturated moisture conditions, they are comparable. For the black coal the wall yield loci for the stainless steel and Tivar surfaces are similar, both exhibiting low friction, this also being the case for the brown coal on the Tivar surface. However as is clearly evident the friction characteristics of brown coal on the stainless steel surface leads to abnormally high friction angles rendering this surface entirely unsuitable as a hopper or chute lining material for brown coal.

Figure 5(c) illustrates the influence of particle size on the wall yield loci. The graphs show the wall yield loci for two particle size ranges of the same black coal on two different wall materials. As indicated, a significant difference occurs for the black mild steel surface, whereas for the bright stainless steel surface the change in particle size range has produced

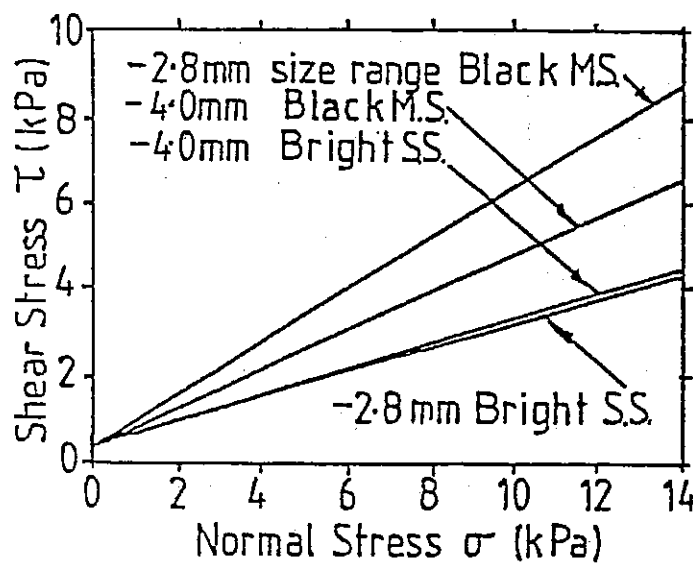
practically no change in the respective wall yield loci. The behaviour depicted in Figure 5(c) may be explained in terms of the interrelation between the particle size distribution and wall roughness.



(a) Wall Yield Loci for Coal on Polished, and Rusted Mild Steel and Stainless Steel.



(b) Wall Yield Loci for Black and Brown Coal on Stainless Steel and Tivar 88.



(c) Wall Yield Loci Showing Effect of Particle Size of Coal on Black Mild Steel and Stainless Steel.

Figure 5 Typical Wall Yield Loci

The adhesive/cohesive characteristics of the W.Y.L. discussed in Section 2.2 is exhibited in the various W.Y.L. shown in Figure 5.

### 3.2 Surface Roughness

Surface roughness is often specified in terms of the centre-line roughness or  $R_a$  number. This is illustrated in Figure 6. The  $R_a$  number (Arithmetic Mean Deviation) of a surface is the arithmetic average of the deviation of a profile from a reference line and is given by

$$R_a = \frac{1}{L} \int_0^L [y(x) - r(x)] dx \quad (4)$$

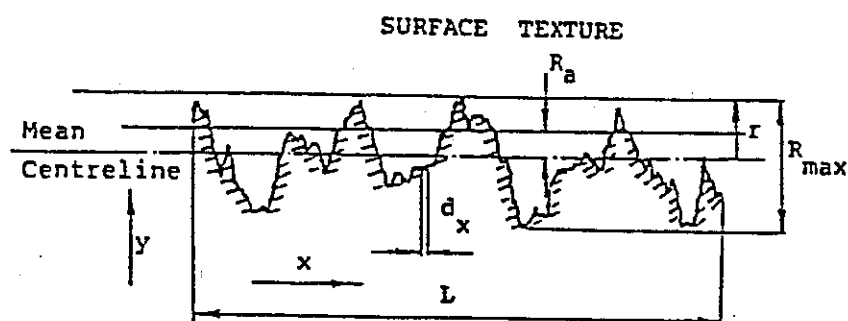


Figure 6 Some Surface Texture Parameters

As shown by Ooms and Roberts [6-9] specification of surface roughness in terms of the mean centre-line roughness index or  $R_a$  number is not sufficient; additional information is required and, for this reason, frequency spectra of wall surface conditions have been adopted for surface analysis.

Figure 7 illustrates, in a diagrammatic way, a typical roughness amplitude versus frequency graph which permits ready correlation with the data on bulk solid particle size distribution. In this way it is possible to assess the interaction between the bulk solid and wall surface with respect to relative sliding motion.

By way of illustration, Figure 8 compares the wall yield loci, surface profiles and surface roughness amplitude frequency spectra for black coal on two samples of stainless steel type 304 with 2B finish. One stainless steel sample is from a 3 mm plate and the other from a 5 mm plate; while both have

the same centre-line or  $R_a$  index, the plates were produced by different rolling processes. It is quite evident that the frequency spectra are quite different and this is reflected in the wall friction characteristics of the 5 mm plate, the rougher surface of the two, being the higher.

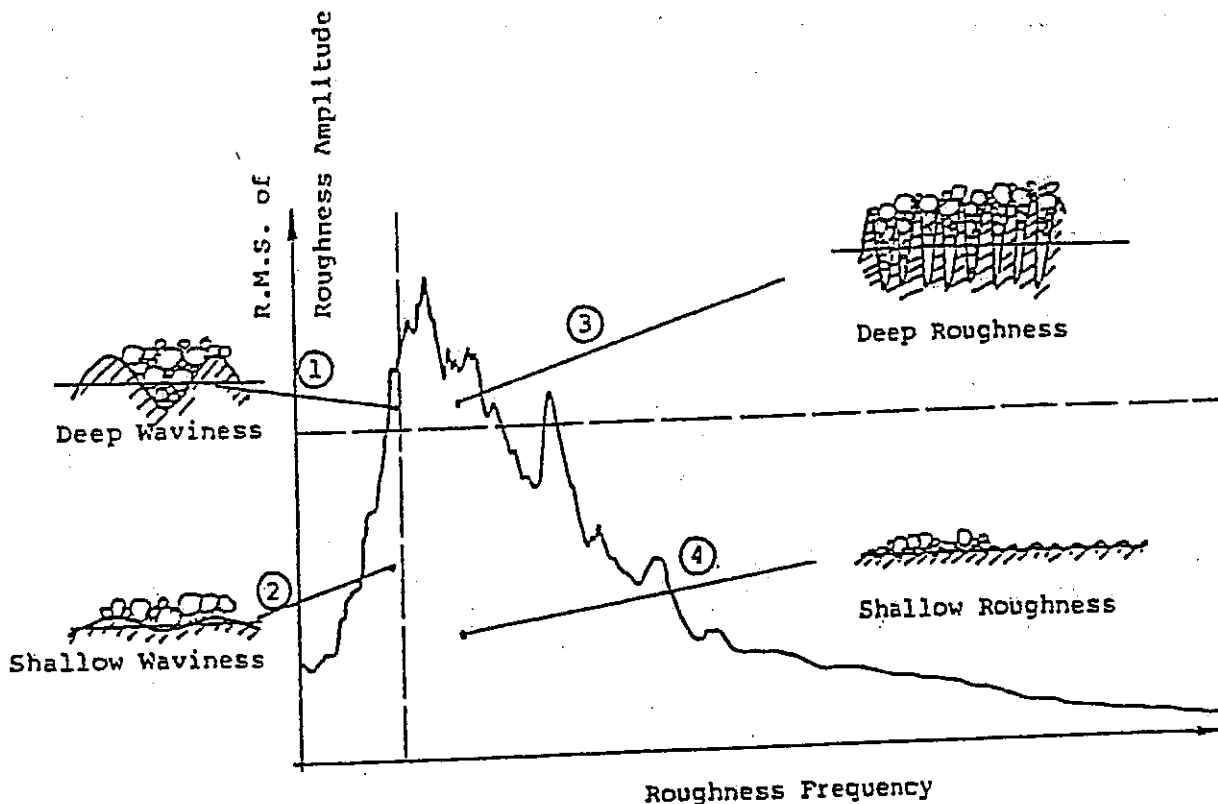


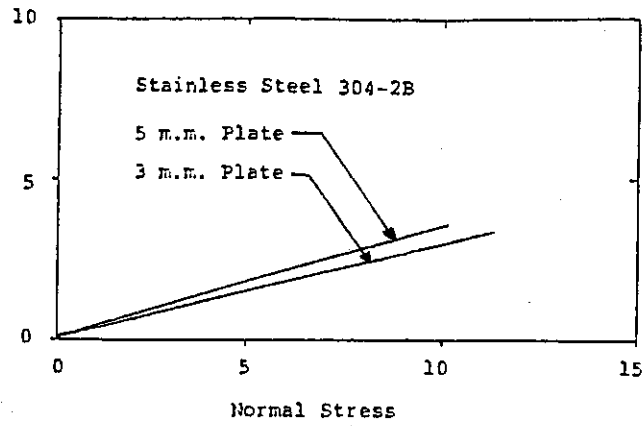
Figure 7 Typical Amplitude Frequency Spectrum of a Random Surface such as Rusted Mild Steel

### 3.3 Influence of Vibrations

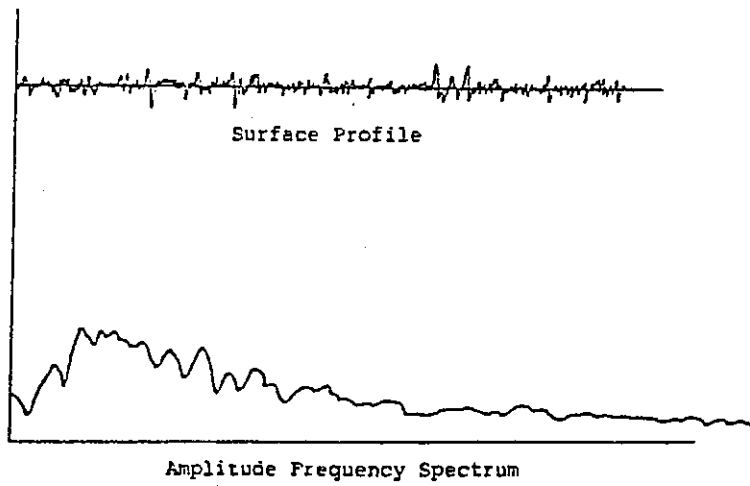
Roberts et al [10-14] have shown that the application of vibrations to a wall surface can significantly reduce wall friction and therefore promote flow. Vibration can also reduce bulk strength, further assisting in promoting gravity flow. The evidence indicates that the best results are achieved by using frequencies of 100 Hertz or higher, and low amplitude.

## 4. SOME ASPECTS OF IMPACT AND ABRASIVE WEAR

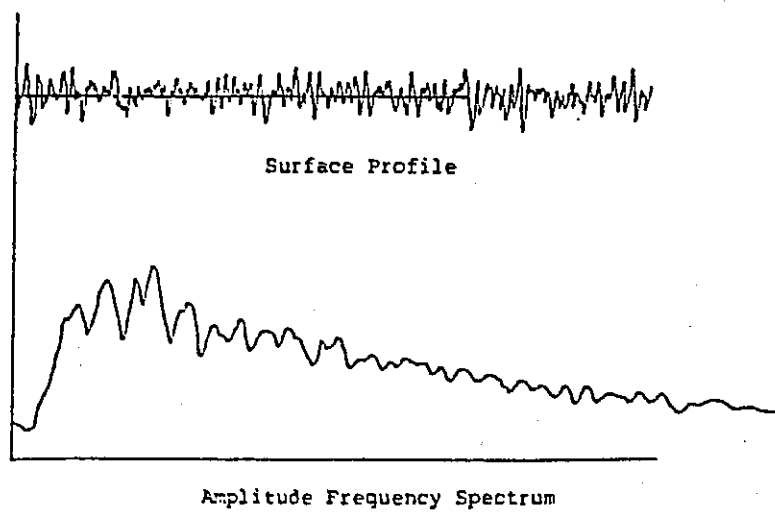
Wear in bulk materials handling plant may result from impact on abrasion or, as is often the case, a combination of both. Erosive wear due to impact occurs when streams of bulk solid particles impinge, usually at medium to high velocity, on inclined surfaces. Typical examples include the intake



(a) Wall Yield Loci for Coal



(b) Stainless Steel 304-2B 3 m.m. Plate



(c) Stainless Steel 304-2B 5 m.m. Plate

Figure 8 Wall Yield Loci, Surface Profile and Roughness Frequency Spectra for Coal on Stainless Steel

end of chutes, baffle or deflector plates at belt conveyor discharge and transfer points, bin and hopper walls subject to impact loading during filling and bends in pneumatic conveyor systems. In the case of the pneumatic conveyor systems, erosive bend wear can be quite substantial due to the high velocity of particles in the air stream particularly in the case of lean phase systems. Wear in bends of pneumatic conveying systems has been the subject of considerable research and the work of Mason, Smith and Mills [15,16] is particularly noteworthy.

Abrasive or rubbing wear occurs when the bulk solid flows along the walls of bins and chutes. Wear in this case is a combination of pressure and rubbing velocity.

Despite the considerable amount of research and investigation into the subject of abrasive wear, there is limited information pertaining directly to the wear in bins and chutes. Johanson and Royal [17] have developed a special abrasive wear apparatus to permit quantitative wear tests to be performed on hopper and chute lining materials. They also analysed the wear in storage bins; the same idea, in conceptual form, was also indicated by Roberts [18]. An overview of friction and wear in bulk handling systems was presented by Roberts et al [19].

It is beyond the scope of this paper to present, in any detail, the characteristics of wear in bulk solids handling plant. Rather, the approach that follows involves the presentation of some basic aspects of the mechanics of wear.

#### 4.1 Impact Wear

Following the work of Finnie [20], Bitter [21,22], Nielson and Gilchrist [23] and Tilly [24], the basic characteristics of impact initiated erosive wear can be summarised as follows:

- . For a brittle material, such as glass, maximum wear occurs when the particles impinge perpendicular to the surface. In this case wear is initiated by crack propagation at the point of impact. For low impact angles, little wear occurs, with the particle glancing off the surface.
- . For ductile materials, such as aluminium alloy, wear increases rapidly as the impact angle increases from zero to around 25° where maximum wear occurs. As the impact angle increases beyond this value, the wear decreases. Wear in this case is a combination of cutting or gouging and local deformation.

- For materials exhibiting a blend of ductile and brittle characteristics, the wear mechanisms involves a combination of the above behaviour.

An indication of the potential for erosive wear can be obtained by examining the energy loss due to impact of impinging particles on an inclined surface. Consider a single particle moving with velocity  $v_1$  impinging on surface at angle  $\theta_1$  as shown in Figure 9.

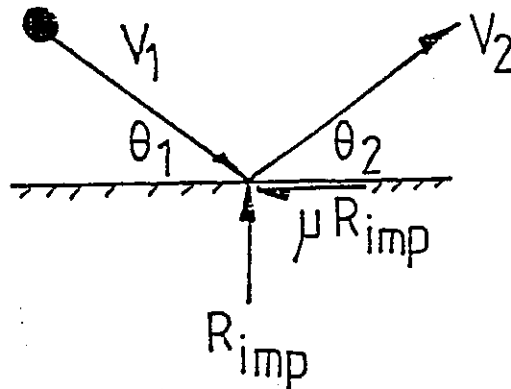


Figure 9 Impact of Particle on Surface

The particle rebounds with velocity  $v_2$  at an angle  $\theta_2$ . The coefficient of friction of the particle in contact with the surface is  $\mu$  and the coefficient of restitution due to normal impact is  $e$ . The impulsive force  $R_{imp}$  is as shown. Based on momentum analysis the final velocity after impact  $v_2$  and angle  $\theta_2$  may be determined. The total loss in energy  $\Delta E$  due to impact expressed as a ratio of initial energy  $E = \frac{1}{2} m v_1^2$  may be shown to be

$$\frac{\Delta E}{E} = 1 - \{e^2 \sin^2 \theta_1 + [\cos \theta_1 - \beta(1 + e) \sin \theta_1]^2\} \quad (5)$$

where  $\beta = \mu = \tan \phi$  for  $\theta \leq (90 - \phi)$  (6)

$$\beta = \tan(90 - \theta) \text{ for } \theta > (90 - \theta) \quad (7)$$

( $\phi$  = friction angle for the surface).

The loss in energy given by equation (5) may be expressed in terms of the impact component and scouring or rubbing component. That is

$$\frac{\Delta E}{E} = \underbrace{1 - \{e^2 \sin^2 \theta_1 + \cos^2 \theta_1\}}_{\Delta E_i} + \underbrace{\{\beta(1+e) \sin^2 \theta_1 - [\beta(1+e) \sin \theta_1]^2\}}_{\Delta s} \quad (8)$$

The form of the energy loss graphs for various values of  $\phi$  and  $e$  are illustrated in Figure 10. The loss in energy represents the total erosion or wear of the surface together with the damage to the particle itself as well as the heat generated. The relative damage to the particle and the surface would depend on a number of factors with the relative hardness of the particle and surface having a significant contribution. The factor  $\beta$  in equation (5) represents the component of the energy loss due to deformation and gouging of the surface, a factor of relevance to ductile materials. As  $\beta \rightarrow 0$  the energy loss curves are equivalent to impact on a hard brittle surface while as  $\beta$  increases the impact becomes more characteristic of ductile behaviour. Figure 11 shows the components of the energy loss of equation (8) expressed in ratio form, the contribution of the energy losses at various impact angles.

### LOSS IN ENERGY DUE TO IMPACT

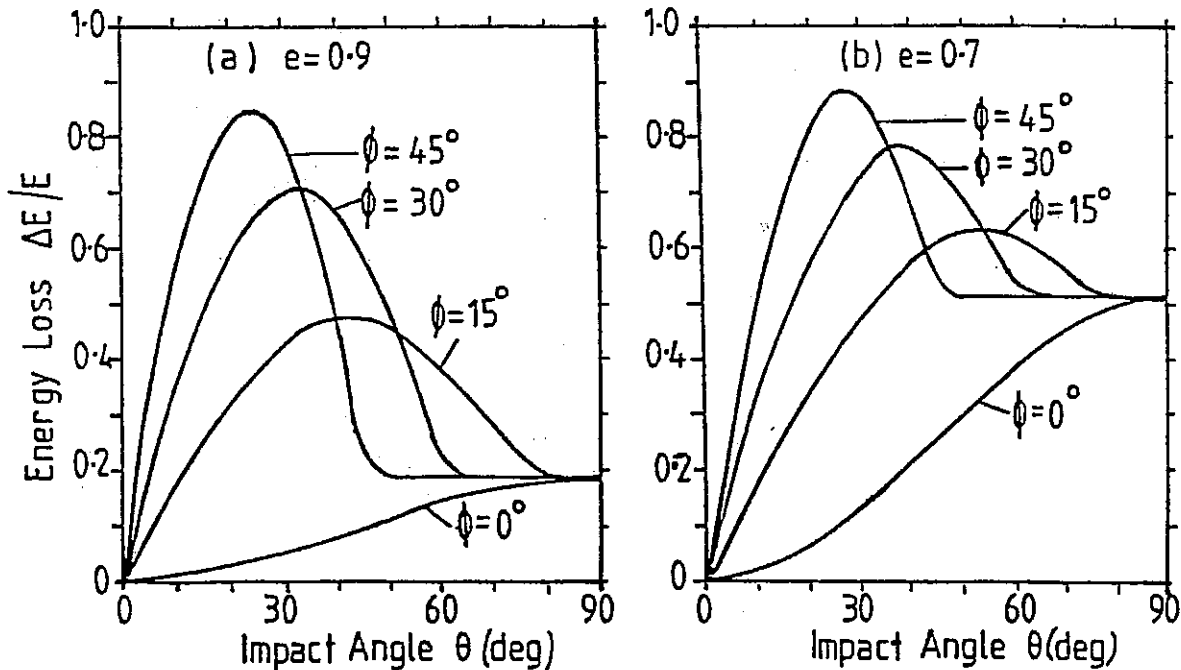


Figure 10 Loss in Energy due to Impact

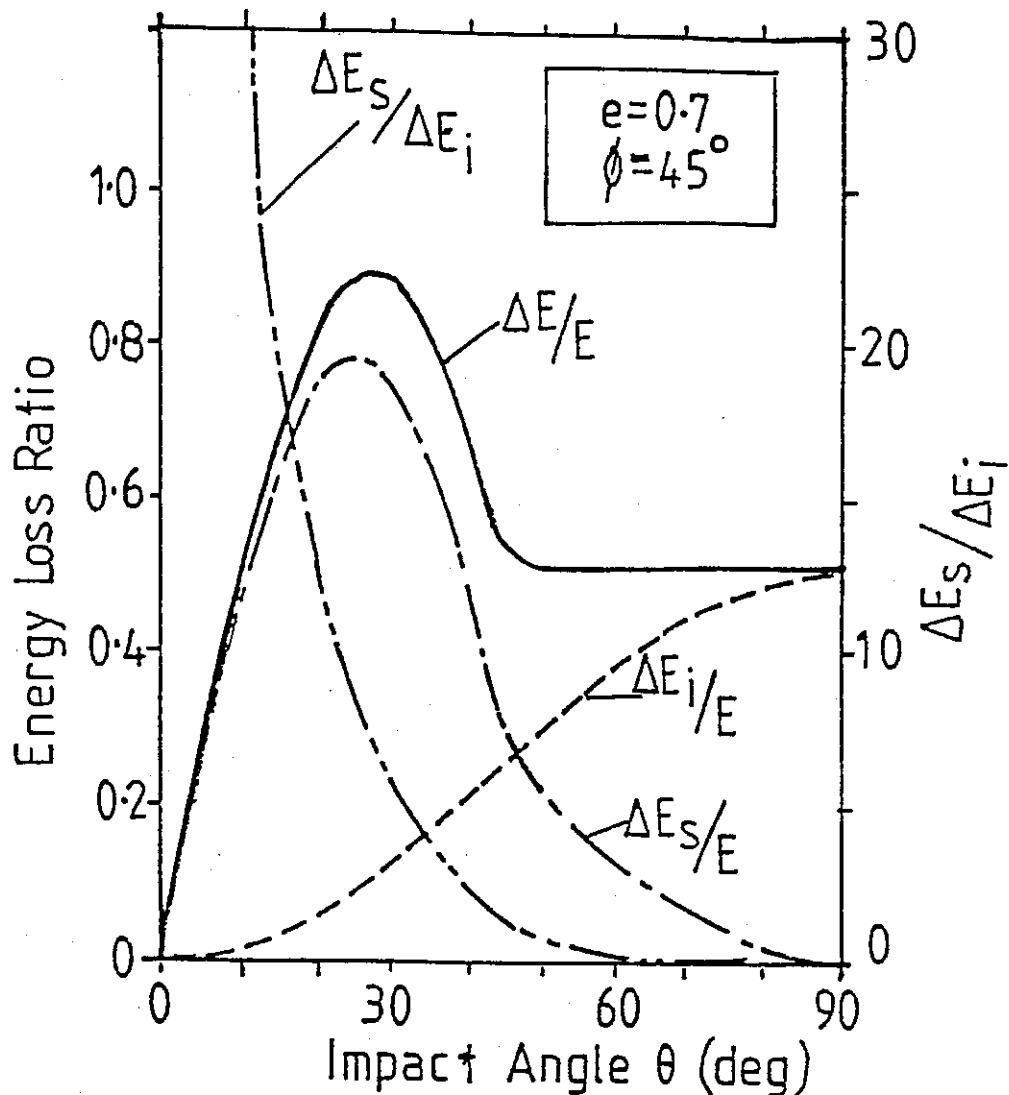
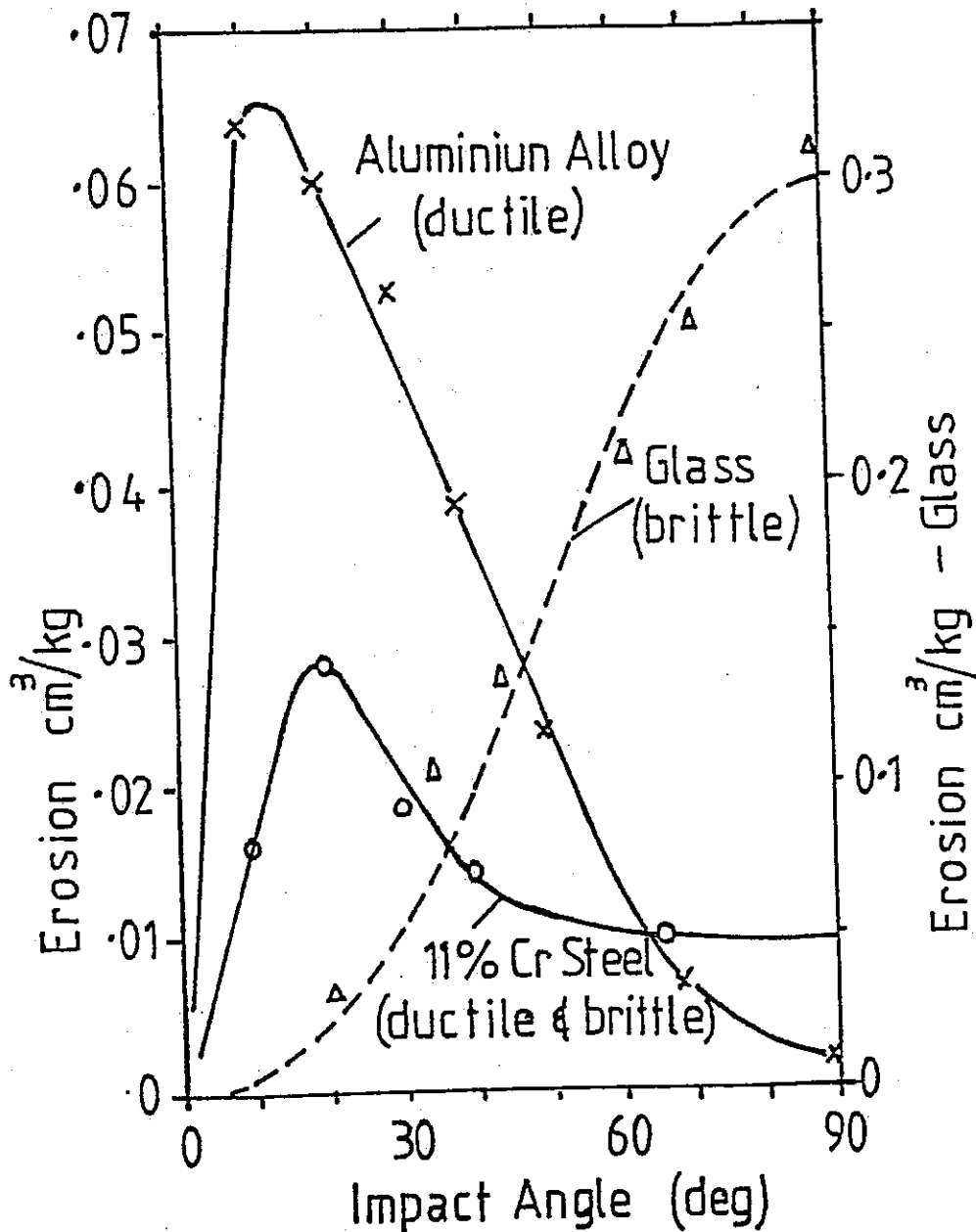


Figure 11 Components of Energy Loss

Although the curves of Figure 10 represent the total energy loss (and hence total damage of surface and particles as well as heat dissipated), the characteristic shapes are similar to those for erosive wear of glass ( $\phi \sim 0$ ) and ductile materials ( $\phi > 0$ ) obtained by Tilly [24], these curves being shown in Figure 12.

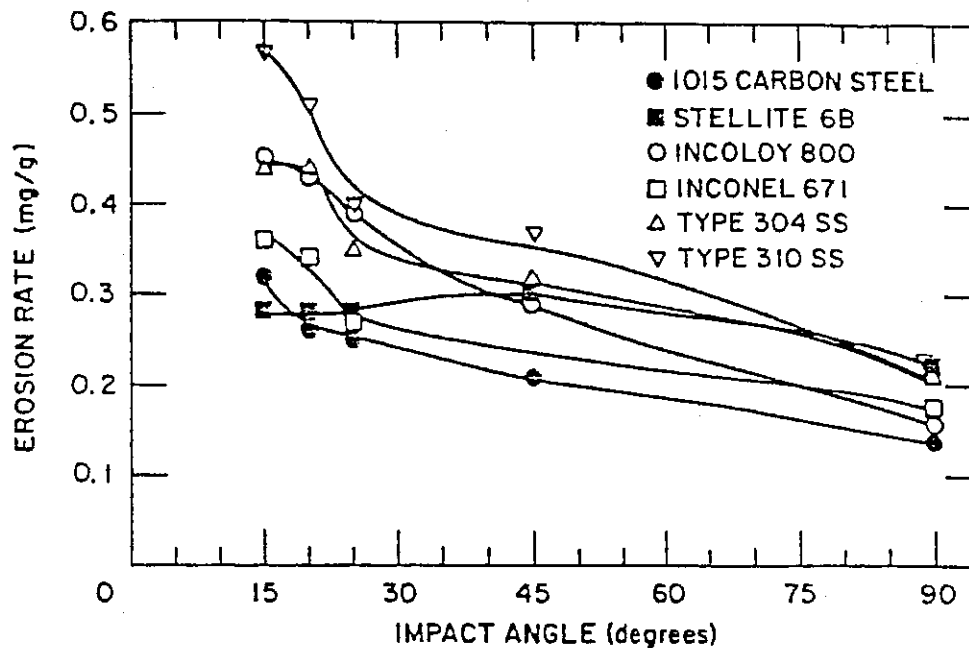
It is to be noted that the maximum erosive wear for glass (at impact angle  $90^\circ$ ) is approximately 4.6 times the maximum erosive wear for Aluminium Alloy (at impact angle  $18^\circ$ ) and 10 times that for 11% Cr. Steel. In terms of the energy loss curves of Figure 10 it would be expected that the erosive wear of glass should be very much lower; however the 'locked up' strain energy in glass and the nature of the crack propagation and chipping resulting from impact accounts for the high relative wear.

A much more detailed analyses of the mechanics of erosive wear has been presented in References [15-24]. Comprehensive wear data for a range of materials has been presented in Reference [31]. By way of illustration, results for some typical wall materials are shown in Figure 13.



Abrasive: Quartz 60-125 $\mu$ m  $v=112$  m/s  
(G.P. Tilly 1969)

Figure 12 Impact Wear Characteristics



<sup>a</sup>Erosion tests were performed at ambient temperatures in air using 60  $\mu\text{m}$   $\text{Al}_2\text{O}_3$  with an impact velocity of 70 m/s at impact angles of 15°, 20°, 25°, 45°, and 90°. [Test time was not given.]

Figure 13 Erosive Wear on Several Alloys as a Function of Impact Angle

Ref: Ondik et al [31] - Tests performed using 60  $\mu\text{m}$   $\text{Al}_2\text{O}_3$  with impact velocity of 70 m/s

#### 4.2 Abrasive Wear

In this case it is assumed that the wear is a direct relation between the normal pressure, the friction coefficient and the rubbing velocity.

$$w = \sigma_w (v_s)^n \tan\phi \quad (9)$$

where

- $\sigma_w$  = normal wall pressure
- $v_s$  = velocity of bulk solid adjacent to wall
- $\phi$  = wall or boundary friction angle
- $n$  = exponent to allow for any rotation of the particles

In the analysis that follows in the next section it is assumed that simple wear occurs for which  $n = 1$ .

## 5. MASS FLOW BIN SPECIFIC WEAR

Typical wall pressure distributions for conical mass flow with the corresponding specific wear profile are presented in Figure 14. The cylindrical sections of the bins are of mild steel with wall friction angle  $\phi = 30^\circ$ , while the hopper section is lined with stainless steel for which  $\phi$  is initially  $20^\circ$ . The bulk material is coal with bulk density  $0.95 \text{ t/m}^3$ .

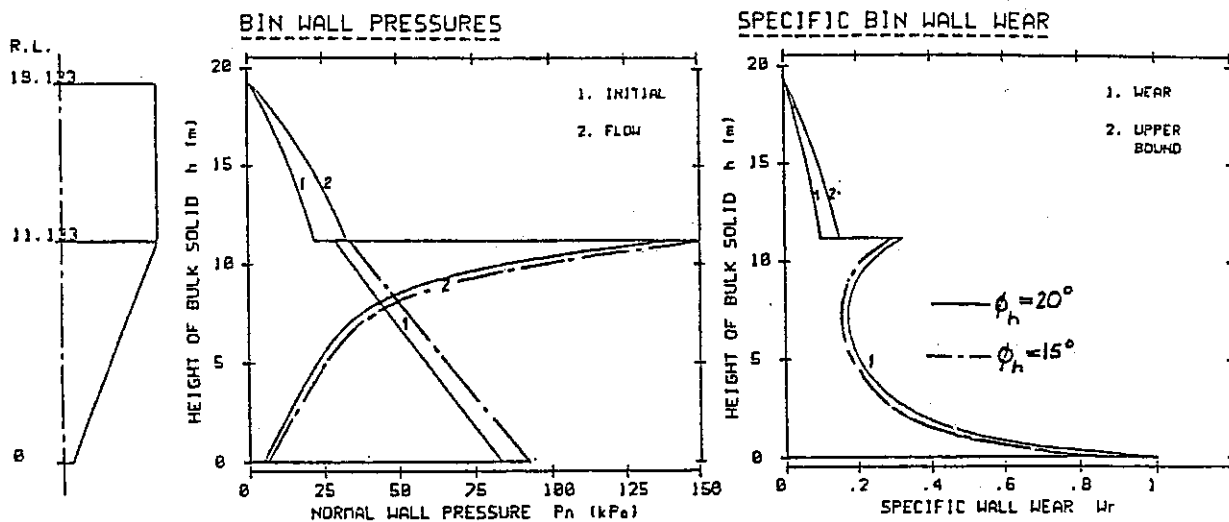


Figure 14 Wall Pressures and Specific Wear for Axi-symmetric Mass Flow Bin  $\phi$  for cylinder =  $30^\circ$ ,  $\phi$  for hopper =  $20^\circ$ ,  $15^\circ$ ,  $\alpha = 22^\circ$ ,  $B = 1 \text{ m}$ ,  $D = 10 \text{ m}$ ,  $\rho = 0.95 \text{ t/m}^3$

### 5.1 Specific Bin Wall Wear

It is difficult to predict, in absolute terms, the likely wear life of bin walls. The wear life will depend on the flow patterns, throughputs and bulk material flow properties, all of which may change over periods of time. Furthermore, for any prediction to be accurate, detailed information on the actual wear characteristics of lining materials would be necessary, but to date such information is often not available. There is a need for reliable test procedures to be established which reproduce the pressure and velocity characteristics of bulk solids in actual gravity flow situations. It is pleasing to note that due to the work of Johanson and Royal [17] some progress on the development of a laboratory wear test for bulk solids has been made. This work provides information on the wear due to fine particles but information on the influence of larger lumps is difficult to acquire.

For design purposes it is possible through the concept of 'specific wear' profiles to indicate zones of high wear in storage bins as illustrated in Figure 14. Information of this type may assist in the selection of lining material thicknesses as well as giving some projections as to the regions of the bin where the lining may, subsequently, have to be replaced.

The specific wear profiles are based on a normalised wear parameter  $W_r$  defined as follows

$$W_r = \frac{\sigma_w v_s \tan\phi}{W_{\max}} \quad (10)$$

where  $W_{\max}$  = maximum estimated value of abrasive wear, the other parameters being as previously defined.

On this basis, the specific wear lies within the range

$$0 < W_r < 1$$

The velocity of bulk solid relative to the wall may be estimated as follows:

$$\text{For cylinder } v_s = v_{av} = \frac{Q_m}{\rho A_c} \quad (11)$$

$$\text{For hopper } v_s = K_v v_{av} = K_v \frac{Q_m}{\rho A_h} \quad (12)$$

where

- $A_c$  = cross-sectional area of cylinder (constant) ( $m^2$ )
- $A_h$  = cross-sectional area of hopper (variable) ( $m^2$ )
- $v_{av}$  = average velocity at any cross-section (m/s)
- $K_v = \frac{v_s}{v_{av}}$

$K_v$  may be determined using the procedures based on the velocity fields presented in Reference [17].

The maximum wear parameter  $W_{\max}$  corresponds to the value  $W_{r(\max)} = 1$  which for a conical hopper usually occurs at the outlet and for a plane flow hopper at the transition. In the case of plane flow bins, any build-up of bulk material at the transition will reduce the wear at this location.

$W_{\max}$  is determined from

$$W_{\max} = \sigma_{w_m} K_{v_m} \frac{Q}{\rho A_m} \tan\phi \left( \frac{N M}{S} \right) \quad (13)$$

where subscript "m" refers to the section of bin where  $W_r = 1$ .

It is to be noted that the analysis has assumed that simple rubbing wear occurs with the wear being directly proportional to the shear stress of the surface and rubbing velocity. The exact functional relationship has yet to be determined.

If the wall friction decreases with increase in wear then the wall pressures will increase. This is illustrated by the 'dotted' curves in Figure 14 where it is assumed that the wall friction in the hopper has decreased to 15°. If the wear is assumed to be linear with increase in pressure, then the reduction in wall friction may more than offset the increase in pressure, leading to a reduction in wear for the same throughput as indicated. However it is known that the wear on some occasions increases non linearly with pressure so that the changing wear pattern is likely to be more complex.

## 6. BIN DESIGN AND OPERATION PRECAUTIONS

### 6.1 Prevention of Impact Damage

The internal surface of the bin, particularly the hopper, should be protected from damage due to impact of materials during filling. The discharge end of the belt conveyors feeding material to the top of the bin should be positioned so that the trajectories followed by lumps of material falling into the bins do not allow contact with the walls. If necessary, an impact baffle plate should be fitted at the conveyor outlet to eliminate the horizontal component of the discharge velocity, thus allowing the material to fall vertically into the bin.

It is most important to always maintain a buffer storage in the bin to prevent damage to the hopper surfaces during filling. Apart from the danger of weakening the hopper walls, any pitting or indentation of the hopper will adversely affect the wall frictional characteristics and this, in turn, will impair the discharge of materials from the bin. To allow adequate protection, the level in the bin should never be allowed to drop below that which is necessary to maintain the hopper section full. For this reason it is important to incorporate a reliable bin level indicator in the bin operating system.

## 6.2 Funnel Flow Bins and Eccentric Discharge

Serious wear problems will arise during funnel flow where the flow channel or pipe is not fully contained in the bulk solid itself but may incorporate part of the hopper or bin wall. Problems of this nature may occur when bins with eccentric discharge are used, particularly when the bin opening is located near a side wall. On other occasions a badly designed feeder may cause material to pile adjacent to the hopper wall. Pipes of this nature give rise to high velocity flow against the wall resulting in accelerated wear.

Often side delivery chutes are incorporated in bins for the purpose of off-loading bulk materials. These create undesirable flow patterns in bins, leading to accelerated wear of the bin wall in the region of the chute intake as well as in the plates above the chute. This wear is caused by both abrasion and impact. Abrasive wear results from the high velocity of the material during chute discharge, the flow following a funnel flow pattern, as indicated in Figure 15(a). After using the chutes the surface of the material in the bin is left sloping steeply downward towards the chute intake. Subsequent filling of the bin will result in large lumps of material bouncing off the surface and striking the bin wall above the chute.

This action accelerates the wear in the plates and, in view of the likelihood of buckling, the bin as a structure will ultimately be weakened.

The eccentric discharge induces a non-uniform pressure distribution as shown in Figure 15(b). Bending is induced and the bin shell is deformed as indicated by the dotted curve. As a result of the vertical loads in the bin due to the material, the bin shell, the conveyor head structure as well as the lateral loads due to the conveyor structure and wind effects, the worn section of the bin wall is prone to localised buckling. The changing wall friction in the wear zone will also lead to changing pressure patterns which could influence the wear and structural integrity of the bin.

It should be noted that despite the fact that side delivery chutes may only be used intermittently, the wear rate during operation is considerable. Side delivery chutes should be avoided; off-loading should preferably be accomplished via a transfer conveyor operating from the main bin discharge. If side delivery chutes are used, such as in an existing installation, it is essential that the bins be lined with wear plates in the region of the chute intakes as well as above the chutes.

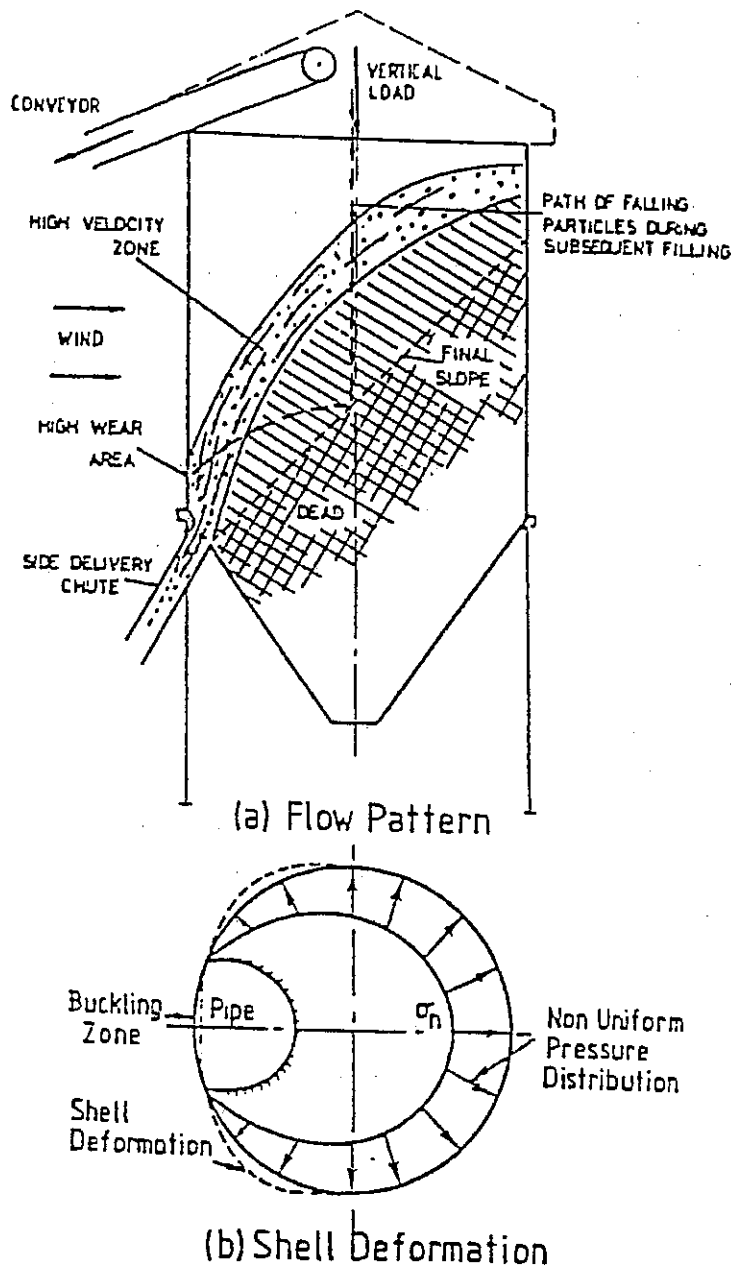


Figure 15 Use of Side Delivery Chutes

## 7. TRANSFER CHUTES AND FEEDERS

### 7.1 Variation of Chute Surface Friction with Bed Depth

Transfer chutes should be designed to ensure that satisfactory flow is obtained without flow blockages. The design of transfer chutes is discussed in some detail in References [3,26,27]. Consideration should be given to the flow properties of the bulk solid and the characteristics of the chute lining material. It has been found, for example, that moist coal can adhere to vertical faces of mild steel chutes eventually causing the chute to become blocked.

When determining chute slope angles account must be taken of the variation of friction angle with change in consolidation pressure or more particularly with change in bed depth.

Figure 16 shows, for a typical coal, the considerably high friction angles that can occur at low bed depths, the decrease in friction angle being significant as the bed depth increases.

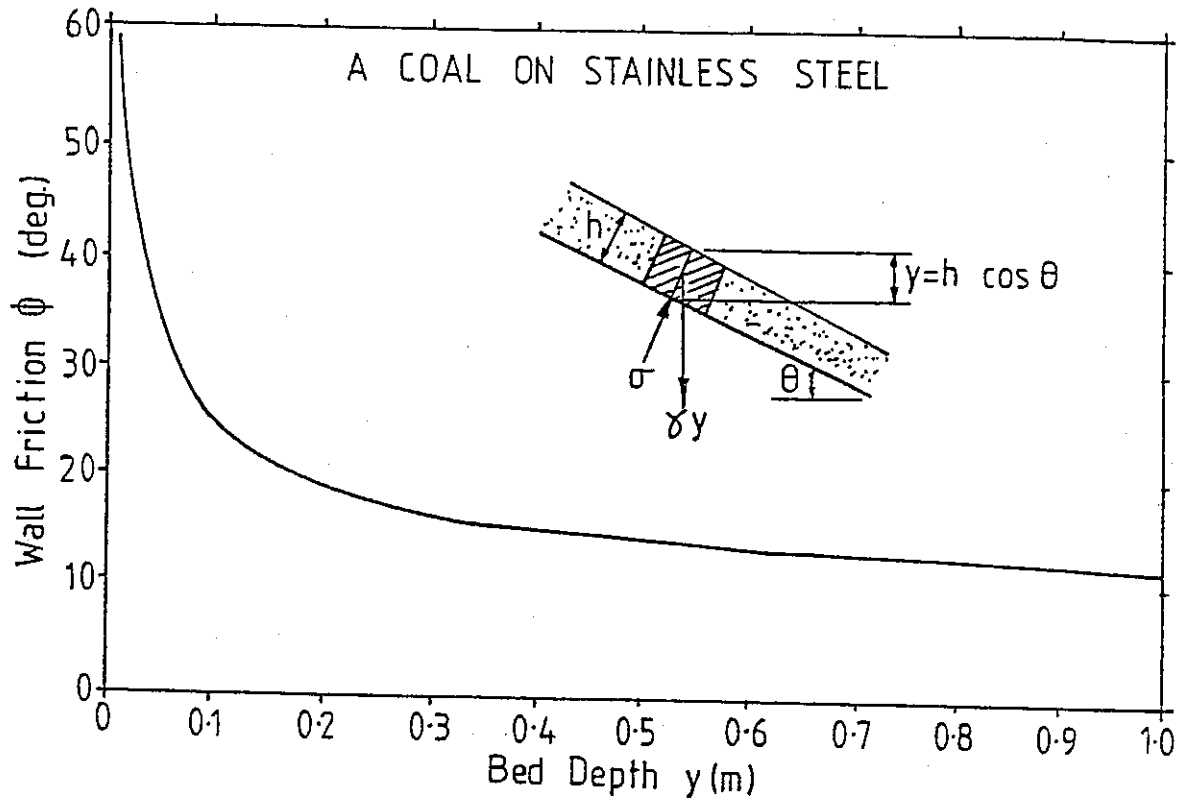


Figure 16 Wall Friction Angle versus Bed Depth for Coal on Stainless Steel

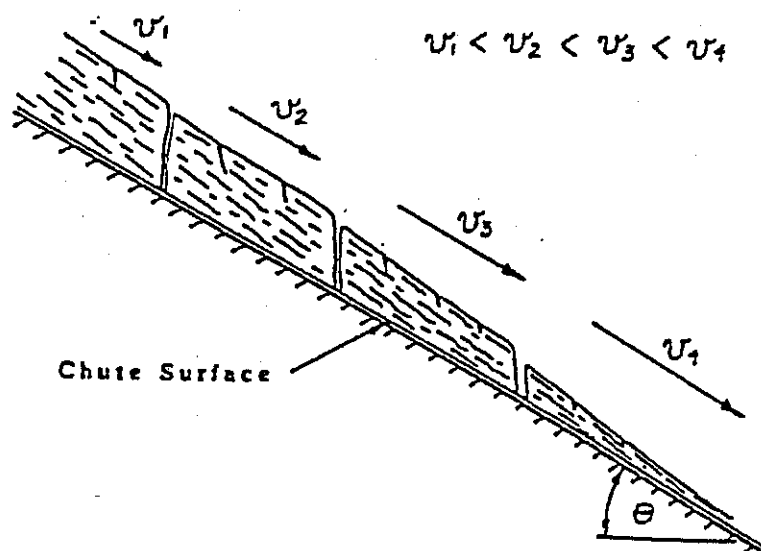


Figure 17 Block-like Flow Down Chute

The slope angle for a chute must be at least  $5^\circ$  larger than the minimum friction angle measured. Often moist bulk solids will adhere initially to a chute surface, but as the bed depth increases, the corresponding decrease in friction angle will cause flow to be initiated. In some cases flow usually commences with a block-like motion of the bulk solid as depicted in Figure 17.

By far the largest component of the drag force in a chute occurs along the chute bottom; the side walls contribute to a lesser extent [26]. Where possible the side walls should be tapered outward with gussets in the corners.

### 7.2 Adhesion in Vertical Chutes or Standpipes

Bulk materials such as coal with high clay contents may adhere to walls of vertical pipes or chutes leading to progressive build-up and flow choking [32]. It is important that the pipe or chute diameter be sufficiently large to cause the bulk solid to fall away from the walls. A proposed simplified methodology is as follows:

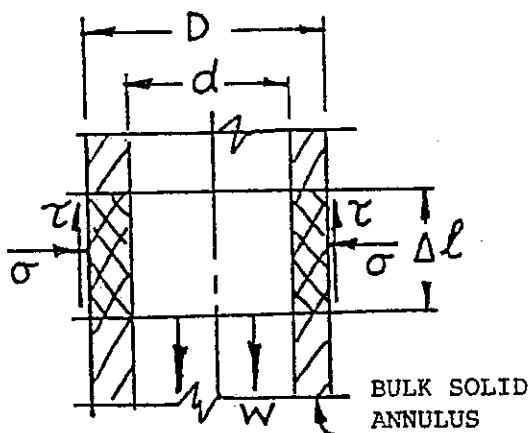


Figure 18 Build up of Bulk Solid in Vertical Chute

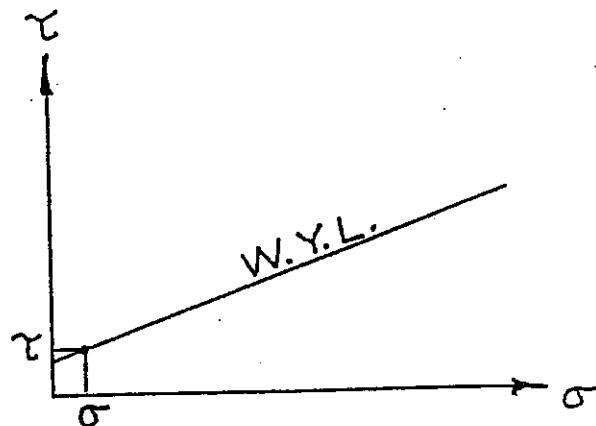


Figure 19 Bulk Solid Wall Yield Locus

Referring to Figures 18 and 19, assuming the weight of bulk solid is just sufficient to cause slip along the wall, the required pipe or chute diameter  $D$  is given by

$$D = \frac{4\tau}{\gamma(1-C^2)} \quad (14)$$

where  $C = d/D$

$\tau$  = shear stress corresponding to pressure  $\sigma$  at wall

$\gamma = \rho g$  = bulk specific weight.

The relationship between  $D$  and  $C$  is shown in Figure 20. Initially when the bulk solid first starts to adhere to the wall  $C \approx 1$ . As build-up occurs,  $C$  reduces, the weight of bulk solid in the Annulus increases and the corresponding pipe diameter  $D$  to allow the bulk solid to fall away decreases. Since the bulk solid will gain bulk strength as the thickness of the annulus increases (i.e. as  $C$  increases) it is important to choose a diameter  $D$  to prevent this happening. For conservative design it is suggested that  $C \leq 0.8$ . Should the annulus grow in thickness thus reducing diameter  $d$ , the greater becomes the strength of the annulus and the greater becomes the possibility for arches ultimately forming.

Figure 20 shows the variation of  $D$  as a function of ratio  $C = d/D$  for various values of  $\tau/\gamma$ . The  $d/D = 0.8$  limit is also shown. Consider, for example, a coal for which  $\tau = 0.35$  kPa corresponding to  $\sigma = 0.5$  kPa, these being typical values for coal with a high montmorellonite clay content; the corresponding bulk density at the low pressure value of  $\sigma$  is  $\rho = 0.71$  t/m<sup>3</sup>. Then  $\tau/\gamma = 0.05$  and from Figure 20, the required minimum pipe diameter corresponding to  $c = 0.8$  is  $D = 0.56$  m.

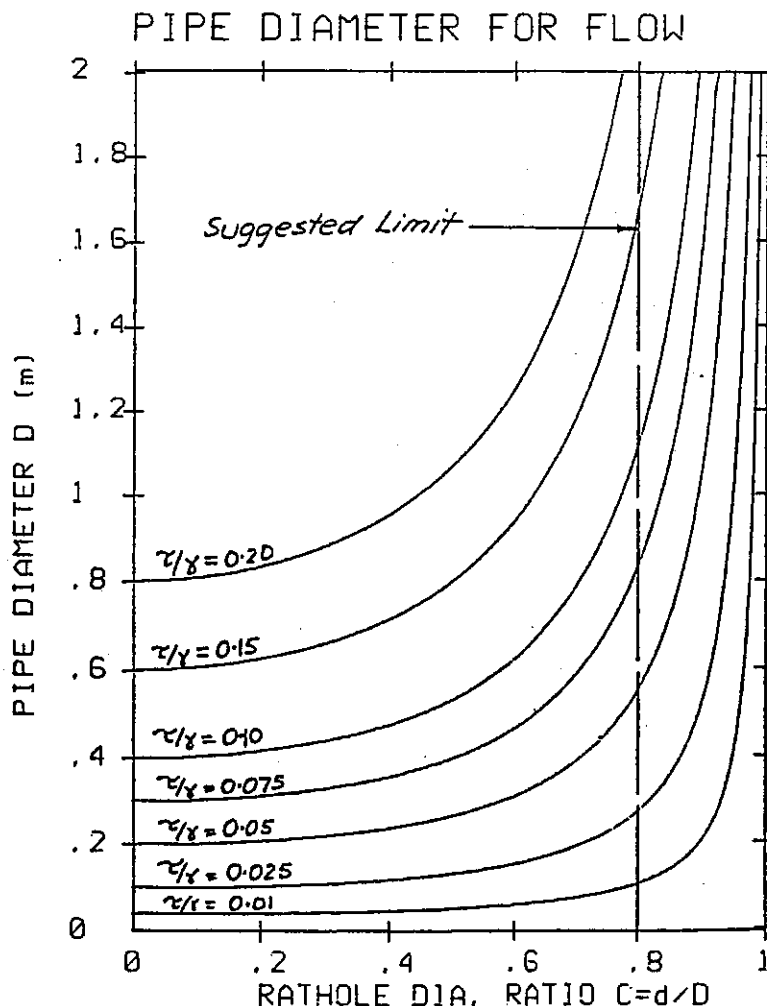


Figure 20 Pipe Diameters for Vertical Chutes as Function of  $c/D$  for Various  $\tau/\gamma$  Ratios

### 7.3 Abrasive Wear in Chutes

For the case of 'fast' flow in chutes [27], where the bulk solid moves as a continuous stream, the abrasive or rubbing wear may be determined as follows:

Consider the general case of a curved chute of rectangular cross-section as shown in Figure 21; an abrasive wear factor  $W_c$  for rubbing against the chute bottom is given by

$$W_c = \frac{F_N v_s \tan\phi}{b \Delta s} \quad (15)$$

where  $F_N$  = normal force (N)  
 $v_s$  = velocity of sliding against chute bottom (m/s)  
 $\phi$  = chute friction angle  
 $b$  = chute width (m)  
 $\Delta s$  = length of element (m)

Now 
$$F_N = \rho b h \Delta s \left[ \frac{v^2}{R} + g \sin\theta \right] \quad (16)$$

$$v_s = K_c v \quad (17)$$

and

$$Q = \rho b h v \quad (18)$$

Hence in (15)

$$W_c = \frac{Q K_c \tan\phi}{b} \left[ \frac{v^2}{R} + g \sin\theta \right] \quad (19)$$

$$W_c \text{ has units of } \left( \frac{N}{ms} \right)$$

In the above equations, the variables not previously defined are

$\rho$  = bulk density (kg/m<sup>3</sup>)  
 $h$  = stream thickness (m)  
 $Q$  = throughput (kg/s)  
 $v$  = average stream velocity at section considered (m/s)  
 $g$  = acceleration due to gravity (m/s<sup>2</sup>)  
 $\theta$  = slope angle of chute measured from vertical.

The factor  $K_c < 1$ .  $K_c$  may be estimated from the results given by Roberts [27]. For 'fast' thin stream flow  $K_c \approx 0.8$ . As the stream thickness increases  $K_c$  will reduce.

Two particular chute geometries are of practical interest, straight inclined chutes and circularly curved chutes, the latter being shown in Figure 21.

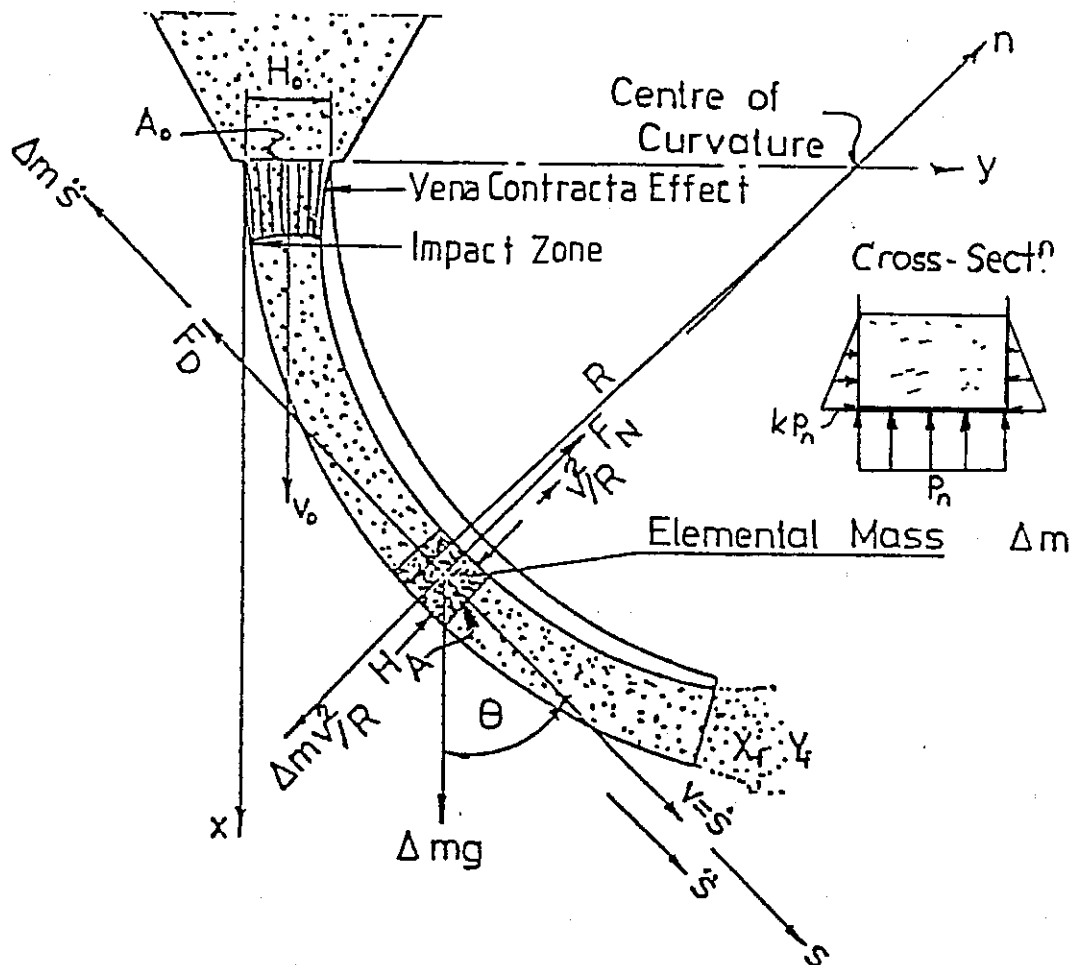


Figure 21 Chute Flow Model

(i) Straight Inclined Chutes

In this case  $R = \infty$  and equation (19) reduces to

$$w_c = \frac{Q K_c \tan \phi g \sin \theta}{b} \quad (20)$$

On the assumption that  $K_c$  is nominally constant when the wear is constant along the chute and independent of the velocity variation.

## (ii) Circularly Curved Chutes

In this case  $R$  is constant and the wear  $W_c$  is given by equation (19). As shown by Roberts [26] the velocity variation around a circularly curved chute may be computed from the following equation:

$$v = \sqrt{\frac{2gR}{4\mu_E^2+1} [\sin\theta (1 - 2\mu_E^2) + 3\mu_E \cos\theta] + e^{-2\mu_E\theta} \left[ v_o^2 - \frac{6\mu_E g R}{4\mu_E^2 + 1} \right]} \quad (21)$$

where  $\mu_E$  = equivalent friction coefficient to allow for sliding against the chute bottom and side walls. Equation (21) assumes  $\mu_E$  is set at a constant average value.

$\mu_E$  may be estimated from

$$\mu_E = \tan\phi \left( 1 + k \frac{h_{av}}{b} \right) \quad (22)$$

where  $h_{av}$  = average height of stream

$k$  = ratio of lateral to normal pressure.

For normal range of applications  $0.4 < k < 1.0$ .

From (18) and (20), the abrasive wear is given by

$$W_c = \frac{Q K_c \tan\phi}{b} \left\{ \frac{2g}{4\mu_E^2+1} [\sin\theta (1 - 2\mu_E^2) + 3\mu_E \cos\theta] + e^{-2\mu_E\theta} \left[ \frac{v_o^2}{R} - \frac{6\mu_E g}{4\mu_E^2+1} \right] + g \sin\theta \right\} \quad (23)$$

To illustrate the wear characteristics of circularly curved chutes the velocity distributions and wear factor  $W_c$  for a particular case is shown plotted in Figure 22. As indicated  $W_c$  is insensitive to chute radius particularly if the initial velocity  $v_o$  is small; the maximum wear occurs at  $\theta$  approximately equal to  $55^\circ$ . In practice, circularly curved chutes need to be terminated at a cut-off angle  $\theta_f$  in order to ensure self-cleaning and non-choking should the flow be interrupted in any way. A straight inclined chute can be fitted to the curved chute if the material is required to be transferred to a location further away. As previously discussed, the wear along the straight chute would be constant.

It is to be noted that the wear plotted in Figure 22 applies to the chute bottom surface. For the side walls the wear will be much less, varying from zero at the stream surface to a maximum at the chute bottom. Assuming the side wall pressure to increase linearly from zero at the stream surface to a maximum value of  $kF_N/b\Delta s$  (see Figure 21) at the bottom, then the average wear on the side walls can be estimated from

$$W_{c \text{ side walls}} = \frac{W_c k}{2 K_c} \quad (24)$$

where  $K_c$  and  $k$  are as defined in equations (16) and (17) respectively. By way of example for  $K_c = 0.8$  and  $k = 0.4$  then the average side wall wear is 25% of the chute bottom surface wear.

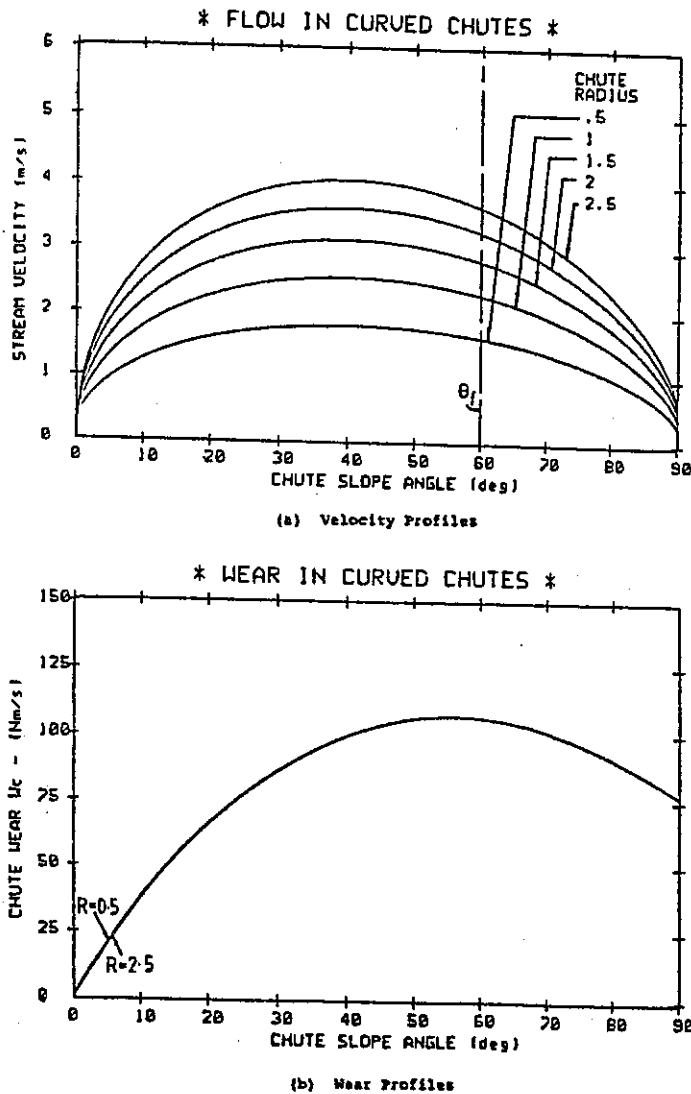


Figure 22 Velocities and Wear Factor for Flow Circularly Curved Chute  
 $Q = 30$  tonne/hr;  $v_o = 0.2$  m/s;  $\rho = 1000$  kg/m<sup>3</sup>;  
 $b = 0.5$  m;  $\mu_E = 0.6$ ;  $\phi = 30^\circ$ .

#### 7.4 Impact Wear in Chutes

Impact wear may occur at points of entry or points of sudden change in direction. The remarks made in Section 4.1 concerning angles of impact should be taken into account in chute design.

#### 7.5 Wear in Feeders

Feeders are used to control the feed rate of bulk solids discharging from storage bins. As emphasised by Roberts et al [28-30] it is most important that the hopper and feeder be designed as an integral unit; a well designed hopper may be prevented from working properly if the feeder is poorly designed and vice versa. Good and bad designs are illustrated in Figure 23.

It is also important that the feed hopper operate under mass flow with the outlet fully active. For this to be achieved it is necessary for the feeder filling capacity to be increased in the direction of feed. Badly designed feeders do not allow for increased filling in the direction of feeding and consequently piping or rat-holing occurs in the hopper leading to accelerated wear of the hopper surface exposed to the flow channel.

In belt and apron feeders caution needs to be exercised in the case of vertical skirts and control gates as these can negate the benefits of tapered outlets. Gates should only be used as flow trimming devices and not for flow rate control; the latter should be achieved by varying the speed of the feeder.

In practice the loads exerted on feeders vary considerably. The loads exerted on feeders following initial filling of the feed bin can vary from 4 to 10 times the loads exerted under flow conditions, the actual variation depending on the feeder and hopper geometry and the bulk solid flow properties. Once flow is initiated the stress field on the hopper switches from a peaked stress field for the filling condition to an arched stress field for the emptying condition, the latter providing wall support for the bulk material leading to a reduced load on the feeder. Even if the feeder is stopped while the bin is still full the load on the feeder stays approximately the same as for the flow condition; the load does not revert to the high initial load. This property, referred to as 'cushioning', is made use of in controlling feeder loads and limiting the feeder power requirements. It also limits the wear of screws, belts and drive components are directly related to the feeder loads.

In the case of feeding bulk solids onto conveyor belts, abrasive wear occurs as the bulk solid slips relative to the belt during the acceleration of

the bulk solid to the belt speed. The wear factor associated with this motion is given by

$$W_b = \frac{Q}{2 b l_b} (v_b - v_m)^2 \left(\frac{N}{ms}\right) \quad (25)$$

- where
- Q = mass flow rate (kg/s)
  - $v_b$  = belt speed (m/s)
  - $v_m$  = velocity of material entering belt (m/s)
  - b = constant width of material on belt
  - $l_b$  = acceleration length (m)

The wear on the belt is proportional to the square of the slip velocity. For belts without skirtplates

$$l_b = \frac{v_b^2 - v_m^2}{2 g \mu} \quad (26)$$

where  $\mu$  = coefficient of friction between bulk solid and belt.

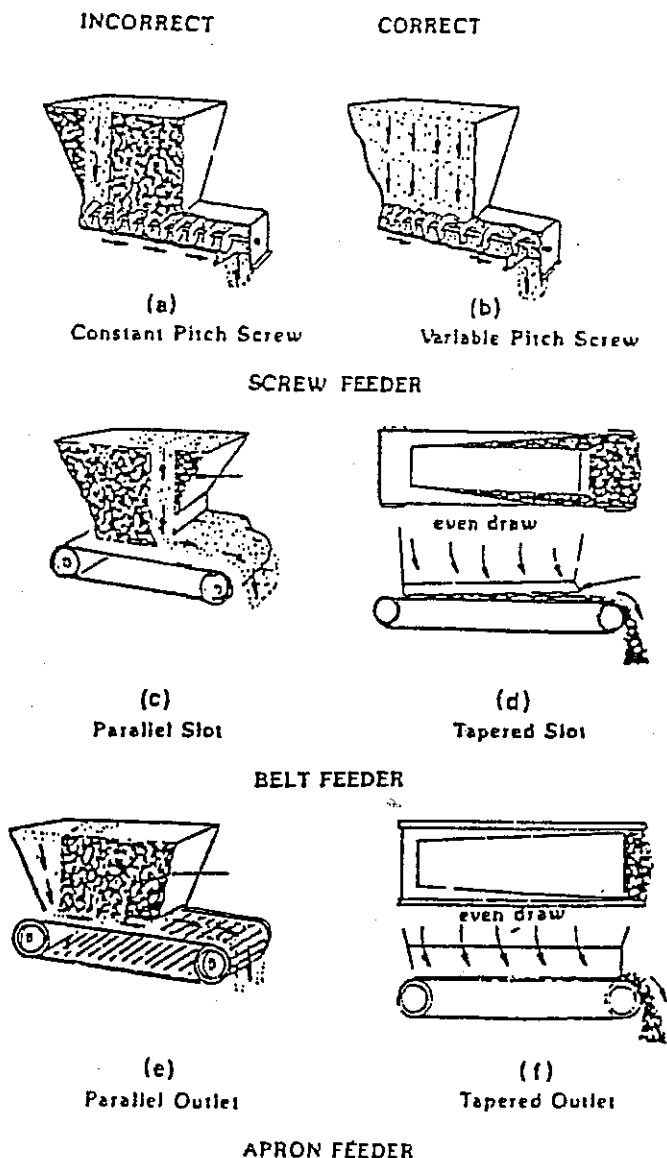


Figure 23 Incorrect and Correct Use of Feeders to Control Discharge

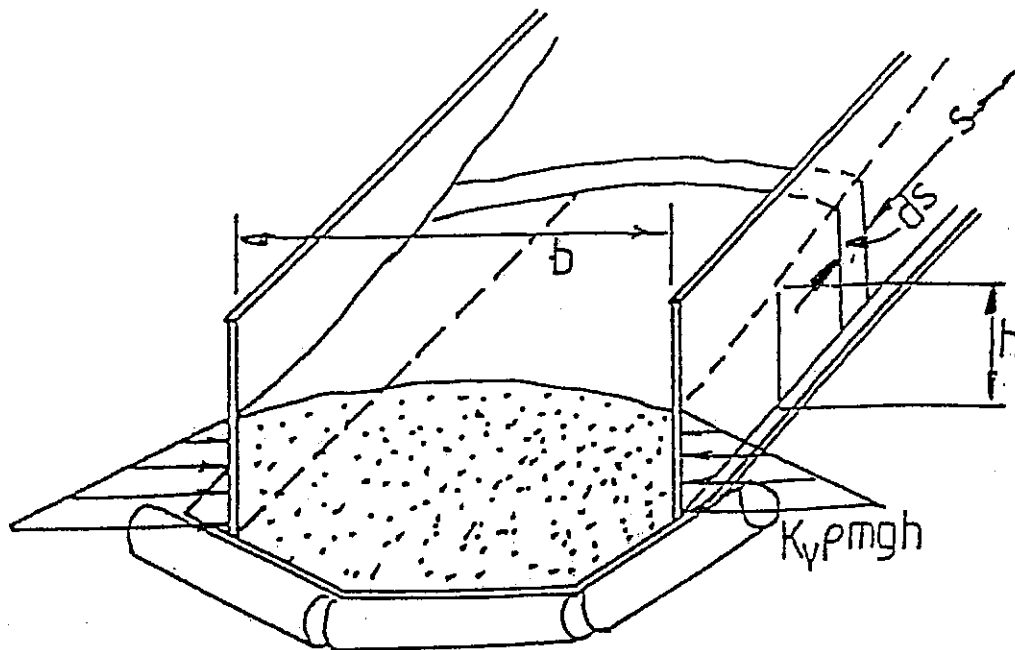


Figure 24 Skirtplates in Acceleration Zone

For belt with skirtplates in feed zone as shown in Figure 24

$$l_b = \frac{1}{\mu g} \left\{ \frac{v_b^2 - v_m^2}{2} + v_m (v_b - v_m) + v_{\min}^2 \ln \left[ \frac{v_b - v_{\min}}{v_m - v_{\min}} \right] \right\} \quad (27)$$

where  $v_{\min}$  is the minimum feed velocity required to achieve required feeding rate.  $v_{\min}$  is given by

$$v_{\min} = \frac{\mu_s k Q}{\mu \rho b^2} \quad (28)$$

where  $\mu_s$  = coefficient of friction for bulk solid on skirtplates.

The other parameters are as previously defined.

#### Example

To illustrate the foregoing, consider the following example.

Coal of density  $\rho = 0.9 \text{ t/m}^3$  is fed onto a conveyor belt at a rate of  $Q = 800 \text{ t/h}$  with an initial velocity of  $v_o = 0.5 \text{ m/s}$ . The conveyor has skirtplates in the acceleration zone. It is assumed that  $\mu_1 = 0.5$ ,  $\mu_2 = 0.4$  and, for conservative design,  $K_v = 1.0$ . The width between skirtplates  $b = 1.0 \text{ m}$ . It is required to determine the acceleration length. The belt speed  $v = 3 \text{ m/s}$ .

From (28)  $v_{\min} = 0.198 \text{ (m/s)}$

From (27)  $l_b = 1.011 \text{ (m)}$

From (25)  $w_b = 687 \text{ (}\frac{\text{N}}{\text{ms}}\text{)}$

Account needs to be taken of the frequency at which each individual belt segment passes through the feed zone. The time for one complete circuit of the belt is

$$t = \frac{2 K_L L}{v_b} \quad (29)$$

where  $L$  = length of conveyor (m)  
 $K_L$  = factor to account for additional length of belting due to such factors as pulley wrap, trippers and tensioning devices.

$$K_L > 2.0.$$

For the acceleration zone the time during which slip occurs is

$$t_s = \frac{l_b}{v_b} \quad (30)$$

## 8. BULK SOLID/CONVEYOR BELT INTERACTION IN RELATION TO BELT CLEANING

### 8.1 Introductory Remarks

Continuous, trouble-free operation of belt conveyors depends to a significant extent on efficient and effective belt cleaning. Yet this still remains one aspect of conveyor performance which continues to present problems. Ineffective belt cleaning results in excess carry-over of bulk material leading to build-up on return idlers and spillage; cleaning and maintenance costs may be considerable.

It is well known that a particular type of cleaning device which performs well in one installation may perform badly in another seemingly similar installation. Furthermore, the performance of contact type cleaning devices, such as scrapers, often deteriorate after short periods of useage rendering the need for adjustments to be made on a regular basis.

There are several methods used in practice for cleaning belts during operation, yet the selection of a particular method or device is usually made without any reference to the belt and bulk material properties and the manner in which these properties are influenced by such factors as variations in moisture content, temperature, type of belt and the surface condition of the belt.

## 8.2 Bulk Solid/Belt Surface Interaction

The interaction of bulk solids and conveyor belts is influenced by the belt surface condition. In particular there is a possible correlation between belt surface roughness and bulk solid particle distribution, particularly where particles can become wedged in the grooves and cracks in the belt surface. These surface defects change as the belt passes around the drive drum as a result of belt contraction due to the reduction in tension. This action tends to aggravate the wedging action and retention of particles on the belt surface. In evaluating belt roughness in relation to belt cleaning, it is important to distinguish between roughness measured along and across the belt. It is roughness along the belt that is of greater concern inasmuch as it is this roughness that the belt cleaner will 'see' the most; carry-over will be greater and belt cleaning efficiency lower if longitudinal roughness is significant.

To illustrate the interaction of bulk solids and conveyor belt surfaces, surface friction versus normal pressure results for lead/zinc ore on new and worn conveyor belts are shown in Figure 25. As indicated, the friction angle and hence the cohesion and adhesion become quite large as the consolidation pressure decreases particularly in the case of the worn belt. It is to be noted that the carry-over of bulk solid on a belt is such that the normal pressure is virtually zero and the cohesion a maximum. The results of Figure 25 clearly indicate that the problems encountered in belt cleaning become more pronounced as belts become worn; not only does the cohesive/adhesive influence become more pronounced, but also the increased roughness leads to a greater potential carry-over.

The surface condition of the two belts referred to in Figure 25 are presented in Figure 26. Figure 26(a) shows the roughness amplitude versus frequency spectrum for the new belt while Figure 26(b) shows the corresponding spectrum for the worn belt. For comparison purposes, the  $R_a$  roughness measurements for both belts are also given. As the results indicate, the worn belt exhibits wear depicted by deep scoring of larger wave length (that is low frequency).

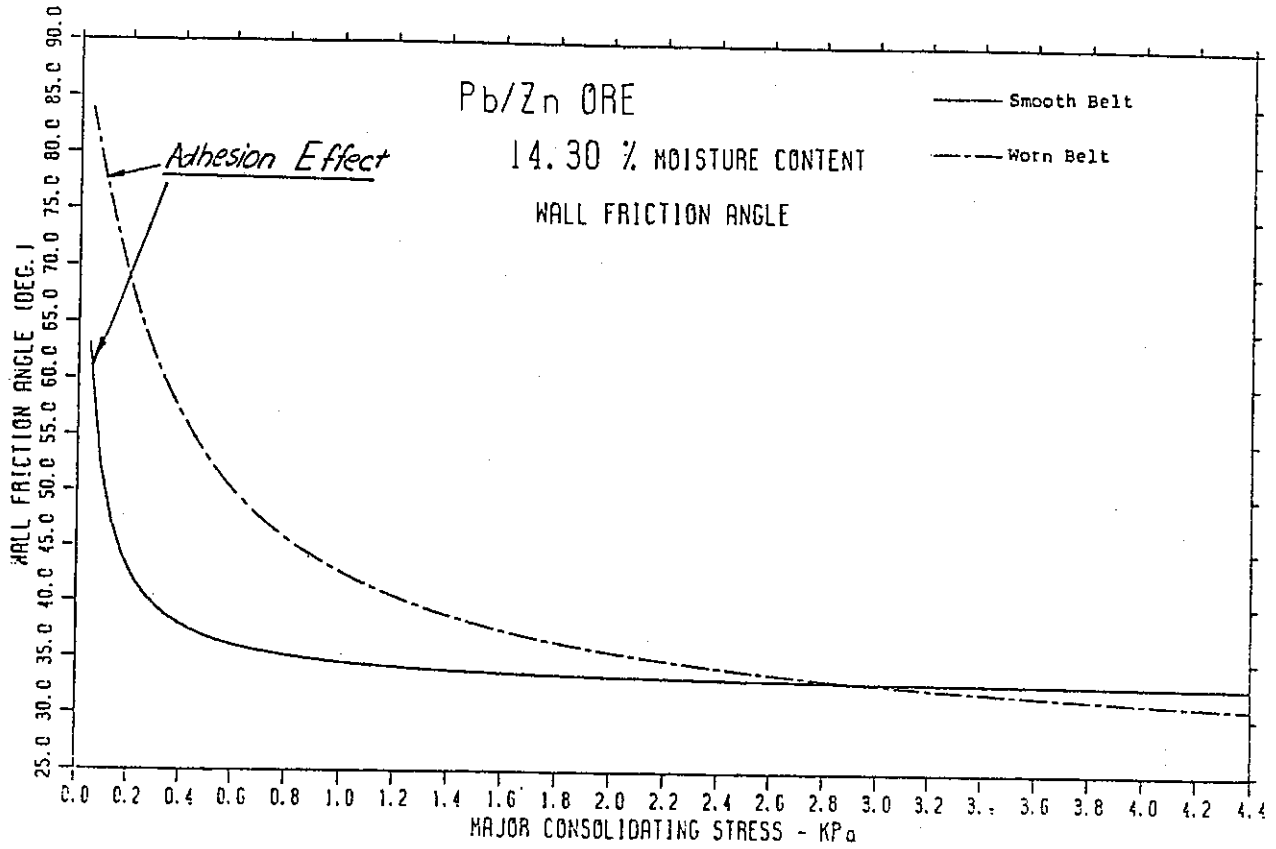


Figure 25 Wall Friction Angle Versus Consolidation Pressure for Lead/Zinc Ore on New and Worn Conveyor Belts

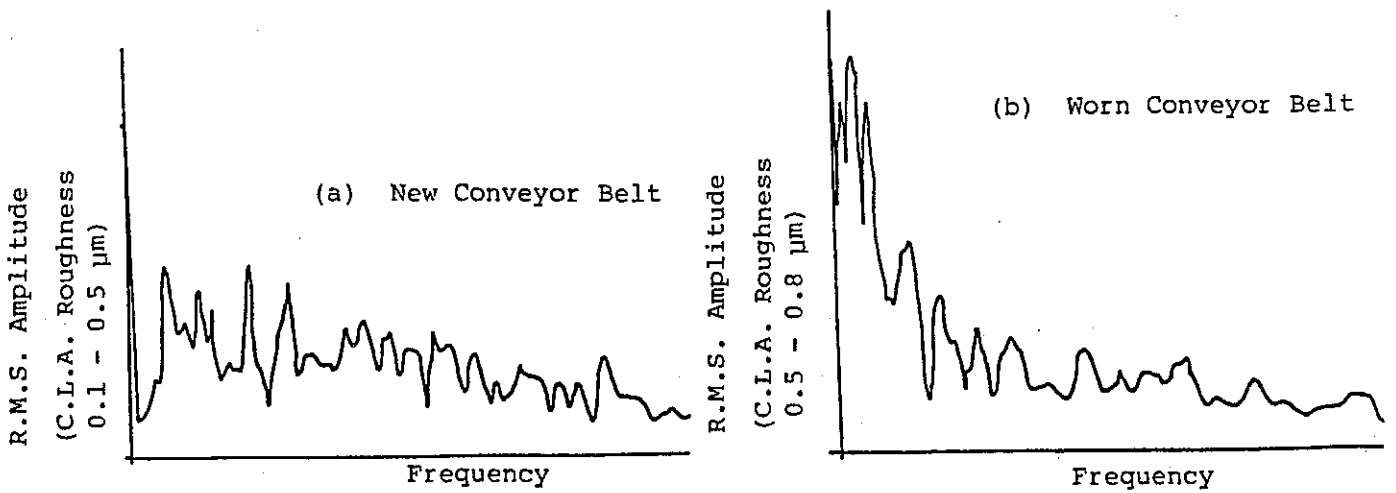


Figure 26 Surface Roughness Spectra for New and Worn Conveyor Belts

### 8.3 Belt Carry-Over and Cleaning Efficiency

The problems associated with belt cleaning, particularly where scraper type cleaners are used, may be assessed by considering the amount of carry-over. Carry-over in tonnes/hour, is given by

$$M_C = 0.0036 m_c B v \text{ (t/hr)} \quad (31)$$

where  $m_c$  = adhesive carry-over ( $\text{gm/m}^2$ )  
 $B$  = belt width (m)  
 $v$  = belt velocity (m/s)

The thickness of material on a belt is given by

$$h = \frac{M_C}{\rho} \text{ (\mu m)} \quad (32)$$

where  $\rho$  = bulk density ( $\text{t/m}^3$ )

Consider, for example, an adhesive carry-over  $m_c = 100 \text{ gm/m}^2$ . For a 1 metre wide belt, a belt speed  $v = 3 \text{ m/s}$  and a bulk density  $\rho = 1 \text{ t/m}^3$  (i.e. coal) the carry-over and thickness are

$$M_C = .0036 \times 100 \times 1 \times 3 = 1.08 \text{ t/h}$$

or  $M_C = 8.64$  tonne per 8 hour shift.

For  $M_C = 100 \text{ gm/m}^2$ , the thickness of particles on the belt is

$$h = \frac{100}{1} = 100 \text{ }\mu\text{m}$$

or  $h = 0.1 \text{ mm}$ .

The foregoing example illustrates that a thickness of only 0.1 mm on the belt can lead to a substantial carry-over which can fall from the belt at return idlers causing an appreciable clean-up problem. The roughness of the belt surface, together with the roughness of scraper blades can result in a significant gap between blade and belt, easily 0.1 mm or more. It is apparent, therefore, that fixed blade scrapers are not effective as belt cleaners.

Belt carry-over in tonnes/hour as a function of adhesive carry-over in  $\text{gms}/\text{m}^2$  is depicted in Figure 27. The depth  $h$  of bulk solid on the belt surface corresponding to various values of  $M_c$  is shown in Figure 28.

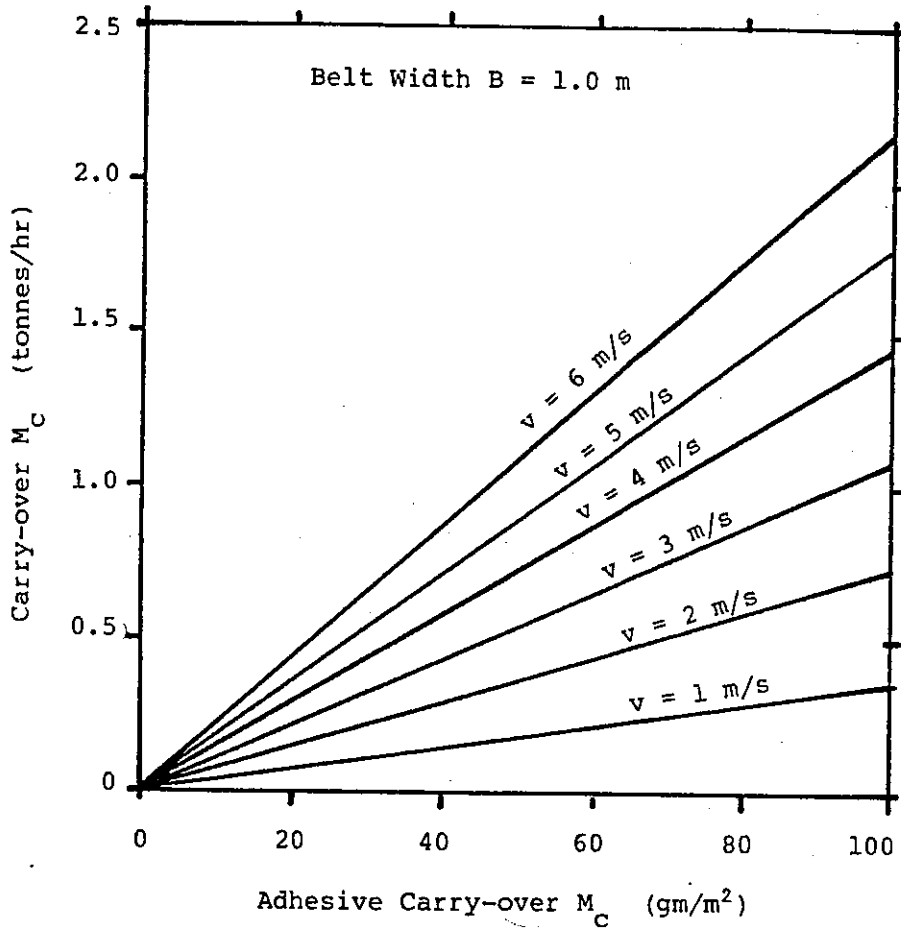


Figure 27. Bulk Solid Carry-over on Conveyor Belts

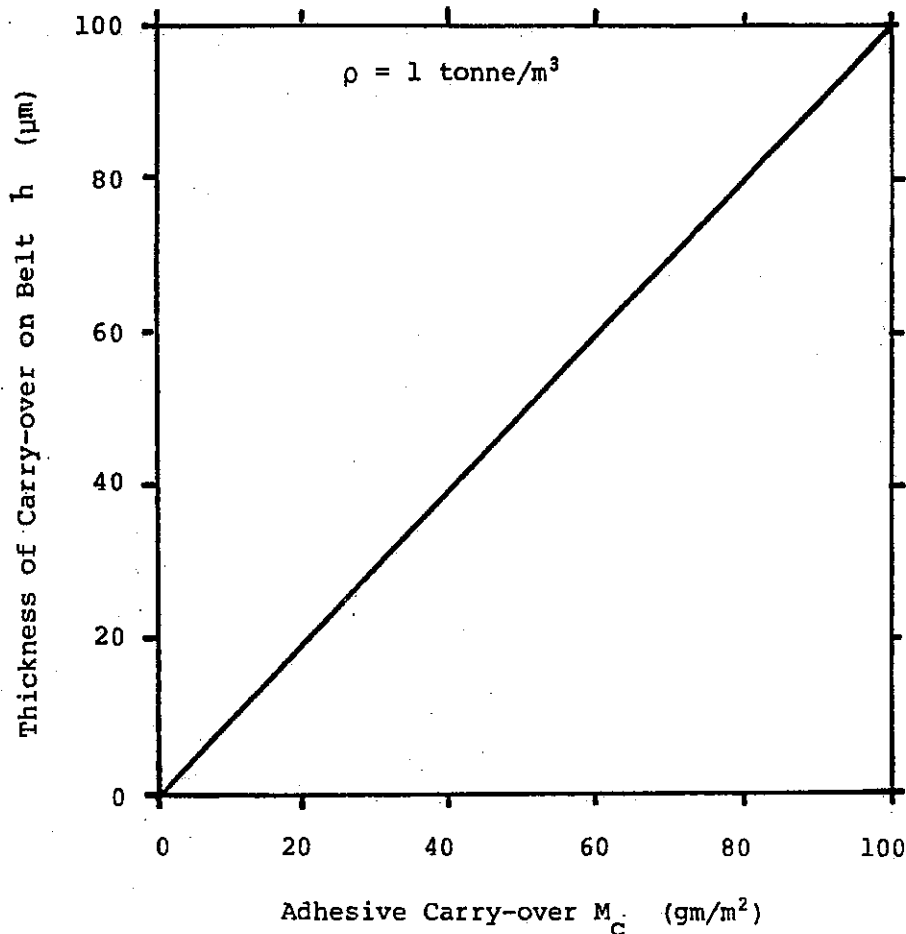


Figure 28 Thickness of Carry-over on Conveyor Belt for  $\rho = 1 \text{ t/m}^3$

Figure 29 shows, schematically, contact between a belt and scraper. The amount of potential carry-over may be assessed as follows:

$$M = 7.2 \times 10^{-3} \eta (R_{a1} + R_{a2}) B_L \rho v \quad (\text{t/h}) \quad (33)$$

where

- $R_{a1}$  = Average centre line roughness for belt ( $\mu\text{m}$ )
- $R_{a2}$  = Average centre line roughness for blade ( $\mu\text{m}$ )
- $\eta$  = Filling factor - function of particle size and shape
- $B_L$  = Effective blade width (m)
- $\rho$  = Bulk density ( $\text{t/m}^3$ )
- $v$  = Belt velocity (m/s)

The amount of carry-over given by (33) will increase as a result of belt and scraper vibrations which will increase the effective clearance between the blade and belt surface.

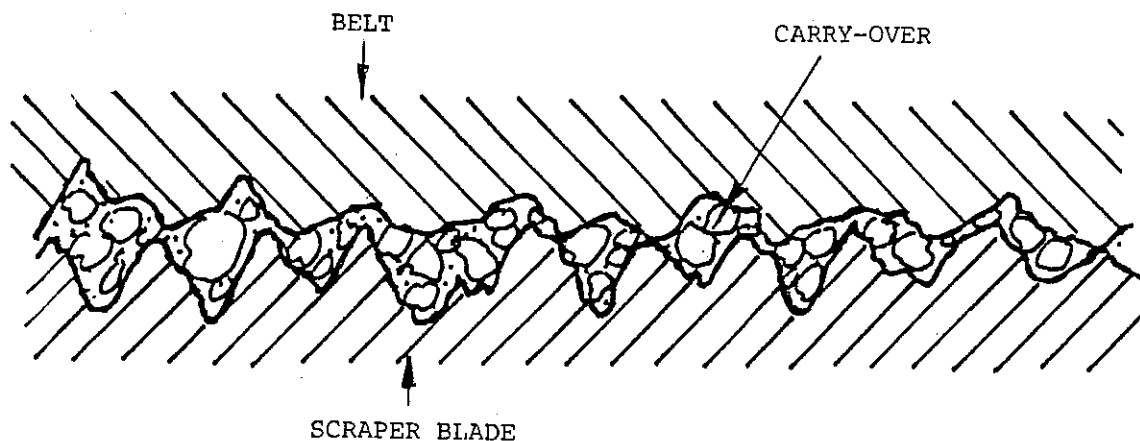


Figure 29 Belt/Scraper Contact Indicating Possible Carry-over

#### 9. CONCLUDING REMARKS

This paper has focused attention on the influence of friction adhesion and wear in the design and performance of bulk solids handling, storage, discharge and belt conveying equipment. Where gravity flow is utilised to discharge bulk solids from bins, through chutes and through feeders, the importance of choosing a wall lining material with low friction and good wear resistance cannot be too strongly emphasised.

As has been indicated wall friction is perhaps the single-most important parameter in the gravity flow of bulk solids. It is essential that the interaction between the bulk solid and the walls of hoppers and chutes be fully understood so that flow patterns can be predicted and correct design be effected.

While, inevitably, reliable gravity flow performance in bins and chutes pre-supposes that wear must occur, based on the theories outlined in this paper, it is possible to predict wear patterns thus permitting due allowance to be made for choice of linings and lining thicknesses at the design stage. There are many examples such as eccentric discharge in bins and badly designed hopper/feeder combinations where wear can be severely aggravated; such 'bad' design should be avoided at all cost. It is possible, with the knowledge now available, to design efficient storage and handling plant which not only give efficient and reliable performance, but also which control the wear of walls and surfaces in a pre-determined way.

In the case of belt cleaning, a knowledge of the adhesion characteristics of bulk solids on belt surfaces is required. In this way the design and

selection of efficient belt cleaning devices that reduce carry-over may be achieved.

#### 10. REFERENCES

1. Jenike, A.W., "Gravity Flow of Bulk Solids". Bul. 108. Utah Engng. Exper. Station, University of Utah, 1961.
2. Jenike, A.W., "Storage and Flow of Solids". Bul. 123. Utah Engng. Exper. Station, University of Utah, 1964.
3. Arnold, P.C., McLean, A.G. and Roberts, A.W., "Bulk Solids: Storage, Flow and Handling". The University of Newcastle Research Associates (TUNRA) Ltd., 2nd Edition, 1980.
4. Roberts, A.W., Arnold, P.C., McLean, A.G. and Scott, O.J., "The Design of Gravity Storage Systems for Bulk Solids". Mechanical Engineering, Transactions, I.E.Aust., Vol. ME7, No. 2, October 1982.
5. Roberts, A.W., Ooms, M. and Scott, O.J., "Practical Design and Operational Aspects of Bulk Solids Storage and Discharge Facilities". Proc. Mill Operations Conf. Aus. Inst. of Mining and Metallurgy, Mt. Isa, Australia, September 1982.
6. Ooms, M. and Roberts, A.W., "The Wall/Bulk Solid Interface Condition and its Effect on Bulk Solids Flow from Storage Bins". Proc. 2nd International Conference on Design of Silos for Strength and Flow, Stratford-Upon-Avon, England, November 1983.
7. Ooms, M. and Roberts, A.W., "Hopper Surface Finish and Friction Interrelation with Respect to Bulk Solids Flow from Storage Bins". Mechanical Engineering, Transactions, I.E.Aust., Vol. ME9, No. 1, April 1984.
8. Ooms, M. and Roberts, A.W., "Interaction between Surface Friction and Roughness in the Gravity Flow of Bulk Solids". Proc. 8th International Congress of Chemical Engineering, CHISA, Prague, Czechoslovakia, September 1984.
9. Ooms, M. and Roberts, A.W., "The Effect of Surface Roughness on the Design and Performance of Gravity Flow Systems". Proc. 10th Anniversary Powder and Bulk Solids Conference, Chicago, U.S.A., May 1985.
10. Roberts, A.W. and Scott, O.J., "An Investigation into the Effects of Sinusoidal and Random Vibrations on the Strength and Flow Properties of Bulk Solids". Powder Technology, 21, pp.45-53, 1978.

11. Roberts, A.W., "The Effects of Vibration on the Strength and Flow Properties of Bulk Solids in Storage Bin Operation". Proc. Intl. Conf. on Design of Silos for Strength and Flow, Univ. of Lancaster, U.K., September 2-4, 1980.
12. Roberts, A.W., Ooms, M. and Scott, O.J., "Vibration Excitation of Bulk Solids in Relation to Storage Bin Design and Performance". Proc. 8th International Conference in Mechanics of Structures and Materials, Newcastle, Australia, August 1982.
13. Roberts, A.W., "Vibrations of Powders and Bulk Solids". Chapter 6, Handbook of Powder Science and Technology, Van Nostrand, 1984.
14. Roberts, A.W., Ooms, M. and Scott, O.J., "Strength and Boundary Friction Characteristics of Bulk Solids in the Presence of Vibrations". Proc. 8th International Congress of Chemical Engineering, CHISA, Prague, Czechoslovakia, September 1984.
15. Mason, J.S. and Smith, B.V., "The Erosion of Bends by Pneumatically Conveyed Suspensions of Abrasive Particles". Powder Technology, Vol. 6, 1972, pp.323-335.
16. Mills, D. and Mason, J.S., "Conveying Velocity Effects in Bend Erosion". Jnl. of Pipelines, Vol. 1, 1981, pp.69-81.
17. Johanson, J.R. and Royal, T.A., "Measuring and Use of Wear Properties for Predicting Life of Bulk Materials Handling Equipment". Bulk Solids Handling, Vol. 2, No. 3, September 1982.
18. Roberts, A.W., "Recent Advances in Research Work on Powder Mechanics and Materials Handling". Proc. International Symposium on Powder Technology '81, Kyoto, Japan, September 1981.
19. Roberts, A.W., Ooms, M. and Scott, O.J., "Surface Friction and Wear in the Storage, Gravity Flow and Handling of Bulk Solids". Proc. International Conference "War on Wear", Wear in Mining and Mineral Extraction Industry, Instn. of Mech. Engrs., Nottingham, Sept. 1984.
20. Finnie, I., "Erosion of Surfaces by Solid Particles". Wear, Vol. 3, 1960, pp.87.
21. Bitter, J.G.A., "A Study of Erosion Phenomena - Part I". Wear, Vol. 6, 1963, pp. 5-21.
22. Bitter, J.G.A., "A Study of Erosion Phenomena - Part II". Wear, Vol. 6, 1963, pp.169-190.

23. Neilson, J.H. and Gilchrist, A., "Erosion by a Stream of Solid Particles". *Wear*, Vol. 11, 1968, pp.111-122.
24. Tilly, G.P., "Erosion Caused by Air Borne Particles". *Wear*, Vol. 14, 1969, pp.64-79.
25. Andrews, B.R., Boundy, B.J. and Roberts, A.W., "Flow Property Analysis, Design and Construction Details for a 2400 Tonne Mass Flow Bin". *Bulk Solids Handling*, Vol. 3, No. 4, November 1983.
26. Roberts, A.W., "An Investigation into the Gravity Flow of Non-Cohesive Granular Materials Through Discharge Chutes". *Trans. A.S.M.E., Jnl. for Engng. in Industry*, Vol. 91, Series B, No. 2, May 1969.
27. Roberts, A.W. and Scott, O.J., "Flow of Bulk Solids Through Transfer Chutes of Variable Geometry and Profile". *Bulk Solids Handling*, Vol. 1, No. 4, December 1981, p.715.
28. Roberts, A.W., "Design and Application of Feeders for the Controlled Loading of Bulk Solids onto Conveyor Belts". *Proc. Belton 2, International Conference on Materials Handling, Johannesburg, South Africa, May 1983.*
29. Roberts, A.W. and Ooms, M., "Hopper Surface Finish and Friction Interrelation with Respect to Bulk Solids Flow from Storage Bins". *Mechanical Engineering Transactions, I.E.Aust.*, Vol. ME9, No. 1, April 1984.
30. Roberts, A.W., Ooms, M. and Manjunath, K.S., "Feeder Load and Powder Requirements in the Controlled Gravity Flow of Bulk Solids from Mass Flow Bins". *Mechanical Engineering Transactions, I.E.Aust.*, Vol. ME9, No. 1, April 1984.
31. Ondik, H.M., Christ, B.W., Shives, T.R., Perloff, A. and Beck, B.A., "Construction Materials for Coal Conversion - Performance and Property Data". Supplement 1, U.S. Dept. of Commerce, National Bureau of Standards, December 1983.
32. Roberts, A.W., Scott, O.J. and Ooms, M., "Examination of Coal Blockage Problem". TUNRA Bulk Solids Handling Research Associates, Report No. R5-84-4116, October 1984.